THE JOURNAL OF BIOLOGICAL CHEMISTRY VOL. 289, NO. 7, pp. 4515–4531, February 14, 2014

The Activity of GAT107, an Allosteric Activator and Positive Modulator of α7 Nicotinic Acetylcholine Receptors (nAChR), Is Regulated by Aromatic Amino Acids That Span the Subunit Interface*

Received for publication, October 3, 2013, and in revised form, December 6, 2013 Published, JBC Papers in Press, December 20, 2013, DOI 10.1074/jbc.M113.524603

Roger L. Papke[‡1], Nicole A. Horenstein[§], Abhijit R. Kulkarni[¶], Clare Stokes[‡], Lu W. Corrie[‡], Cheol-Young Maeng[‖], and Ganesh A. Thakur[¶2]

From the [‡]Department of Pharmacology and Therapeutics, University of Florida College of Medicine, Gainesville, Florida 32610, the [§]Department of Chemistry, University of Florida, Gainesville, Florida 32611, the [¶]Department of Pharmaceutical Sciences and Center for Drug Discovery, Northeastern University, Boston, Massachusetts 02115, and [‖]SK Biopharmaceuticals, 305-712 Daejeon, Korea

Background: Nicotinic acetylcholine receptors are activated by agonists at an orthosteric site and modulated by ligands at allosteric sites.
Results: We identify amino acids required for the coupling between orthosteric and allosteric sites.
Conclusion: Allosteric activation can occur even when the orthosteric binding site is nonfunctional.
Significance: Insights are provided into the cooperative functions of orthosteric and allosteric activators of the α7 nAChR.

GAT107, the (+)-enantiomer of racemic 4-(4-bromophenyl)-3a,4,5,9b-tetrahydro-3*H*-cyclopenta[c]quinoline-8-sulfonamide, is a strong positive allosteric modulator (PAM) of α7 nicotinic acetylcholine receptor (nAChR) activation by orthosteric agonists with intrinsic allosteric agonist activities. The direct activation produced by GAT107 in electrophysiological studies is observed only as long as GAT107 is freely diffusible in solution, although the potentiating activity primed by GAT107 can persist for over 30 min after drug washout. Direct activation is sensitive to α7 nAChR antagonist methyllycaconitine, although the primed potentiation is not. The data are consistent with GAT107 activity arising from two different sites. We show that the coupling between PAMs and the binding of orthosteric ligands requires tryptophan 55 (Trp-55), which is located at the subunit interface on the complementary surface of the orthosteric binding site. Mutations of Trp-55 increase the direct activation produced by GAT107 and reduce or prevent the synergy between allosteric and orthosteric binding sites, so that these mutants can also be directly activated by other PAMs such as PNU-120596 and TQS, which do not activate wild-type α7 in the absence of orthosteric agonists. We identify Tyr-93 as an essential element for orthosteric activation, because Y93C mutants are insensitive to orthosteric agonists but respond to GAT107. Our data show that both orthosteric and allosteric activation of α7 nAChR require cooperative activity at the interface between the subunits in the extracellular domain. These cooperative effects rely on key aromatic residues, and although mutations of Trp-55 reduce the restraints placed on the requirement for orthosteric agonists, Tyr-93 can conduct both orthosteric activation and desensitization among the subunits.

The concept of ligand-gated ion channels as mediators of the transduction of chemical signals at synapses into electrical signals was introduced with the characterization of the nicotinic acetylcholine receptors (nAChR)[3] at neuromuscular junctions. Like all nAChR, muscle-type receptors are pentameric complexes of subunits, and like most nAChR, they contain both α-type and non-α-type subunits that form specialized binding sites for the natural agonist acetylcholine (ACh) and chemical analogs such as nicotine. Such heteromeric nAChR mediate synaptic transmission through autonomic ganglia and have a variety of effects in the central nervous system, although usually not through point-to-point synaptic transmission.

The evolutionary precursors of heteromeric nAChR were pentamers of identical α-type subunits (1), and the predominant nAChR subtype that retains this ancestral feature is the homopentameric α7 nAChR. α7 nAChR lack numerous specializations that evolved for synaptic transmission. They are relatively inefficient at generating ion channel currents, and they lack specializations that would make them strictly "acetylcholine receptors" because they are also activated by the ACh precursor choline (2). The specialized ACh-binding sites of heteromeric nAChR, of which there are two per pentamer, convert to a conformation with very high affinity for ACh and other agonists once the receptor has "desensitized" in

* This work was supported, in whole or in part, by National Institutes of Health Grants GM57481 (to R. L. P.) and DA027113 (to G. A. T.).
[1] To whom correspondence may be addressed: Dept. of Pharmacology and Therapeutics, College of Medicine, University of Florida, Academic Research Bldg., Rm. R5-234, P. O. Box 100267, 1200 Newell Dr., Gainesville, FL 32610. Tel.: 352-392-4712; Fax: 352-392-3558; E-mail: rlpapke@ufl.edu.
[2] To whom correspondence may be addressed: Dept. of Pharmaceutical Sciences and Center for Drug Discovery, Northeastern University, Boston, MA 02115. Tel.: 617-373-8163; E-mail: g.thakur@neu.edu.

[3] The abbreviations used are: nAChR, nicotinic acetylcholine receptor; ACh, acetylcholine; PAM, positive allosteric modulator; MLA, methyllycaconitine; TQS, 4-(1-naphthyl)-3a,4,5,9b-tetrahydro-3*H*-cyclopenta[c]quinoline-8-sulfonamide; A, orthosteric agonist; P, PAM; G, GAT107; 4BP-TQS, 4-(4-bromophenyl)-3a,4,5,9b-tetrahydro-3*H*-cyclopenta[c]quinoline-8-sulfonamide.

regard to ion channel activation. Homomeric α7 nAChR have five agonist-binding sites per receptor, and with high levels of occupancy of these sites, α7 receptors also desensitize, although the binding sites do not significantly change their affinity for agonist, allowing the receptors to readily return to their resting conformation (3).

Consistent with their "ancestral" character, α7 receptors are found in both neuronal and non-neuronal cells such as macrophages (4). It is unclear that the α7 receptors in non-neuronal cells are capable of ion channel activation, but it has been amply demonstrated that they mediate other forms of signal transduction (5). Presently, α7 receptors are being pursued as therapeutic targets for diverse indications such as Alzheimer disease, schizophrenia, and inflammatory diseases such as arthritis and asthma. However, it is unclear whether drugs optimized for these indications will work upon the receptors in the same ways, and it has been proposed that some α7-mediated effects, such as those related to cognition, require ion channel activation, although other functions may be ion channel-independent (6, 7).

nAChRs are allosteric proteins (8), and the conformational equilibrium among the resting, activated (*i.e.* conducting), and desensitized states is affected by the binding of agonists such as ACh to the orthosteric site as well as other ligands to allosteric sites. The first generation of drugs selectively targeting α7 receptors were agonist analogs presumed to bind at the same sites as ACh. Although there has been some limited success at developing such drugs therapeutically (9–11), an alternative approach has been to develop positive allosteric modulators (PAMs) (12) that appear to have selectivity for α7, at least in part, because they can destabilize the forms of desensitization that are unique to α7, and in the absence of the PAM, the desensitized state(s) profoundly limit the probability of ion channel activation (3). PAMs have been hypothesized to bind at allosteric sites within the transmembrane domains of the receptor, at a distance from the "orthosteric" site, which binds ACh and other agonists and is located in the extracellular domains at the interface between subunits (13).

PAMs may profoundly increase ion channel activation and may also impact other forms of signaling as well (14–18). By definition, true PAMs bind at secondary sites and enhance receptor activation by orthosteric agonists. Type II PAMs are agents that are effective at producing both transient and prolonged increases in channel activation, with the long term effects associated with the destabilization of desensitized states (19). PNU-120596 is one of the most well studied type II PAMs; however, a new class of drugs was recently discovered based on structural modifications of an alternative type II PAM, TQS. 4BP-TQS can produce α7 ion channel activation without the requirement of an orthosteric agonist (20), making it the prototype for "ago-PAMs." We have previously identified (21) the active stereoisomer of 4BP-TQS, GAT107 (compound 1b, the (+)-enantiomer of racemic 4BP-TQS with 3a*R*,4*S*,9b*S* absolute stereochemistry). The identification of GAT107 as a molecule that can both function as a direct (allosteric) activator of the channel and as an allosteric modulator of concurrent or subsequent orthosteric agonist-evoked responses (21) suggests it as a tool to dissect the interaction between the orthosteric and allosteric binding sites of the receptor. To do this, we conducted a systematic analysis of the multiple forms of GAT107 activity and supplemented that analysis with the study of mutants known to alter orthosteric activation. In this work, we characterize three forms of GAT107 activity as follows: direct allosteric activation, direct allosteric modulation, and a primed form of potentiation based on long lasting priming of the receptor presumably via a GAT107/receptor-bound state. Some of these activities require coupling between the orthosteric and allosteric binding sites. We identify amino acids on either side of the subunit interface that proscribe the orthosteric binding site and control this coupling, and we describe mutations that can modify or eliminate that coupling.

MATERIALS AND METHODS

Chemicals—Solvents and reagents were purchased from Sigma. Cell culture supplies were purchased from Invitrogen. Hanks' balanced saline solution (I methyllycaconitine) contained (in mM) the following: 1.26 $CaCl_2$, 0.493 $MgCl_2$, 0.407 $MgSO_4$, 5.33 KCl, 0.441 KH_2PO_4, 4.17 $NaHCO_3$, 137.93 NaCl, 0.338 Na_2HPO_4, and 5.56 D-glucose. PNU-120596 (1-(5-chloro-2,4-dimethoxyphenyl)-3-(5-methylisoxazol-3-yl)-urea) was synthesized by Dr. Jingyi Wang and Kinga Chojnacka as described previously (3). GAT107 ((3a*R*,4*S*,9b*S*)-4-(4-bromophenyl)-3a,4,5,9b-tetrahydro-3*H*-cyclopenta[c]quinoline-8-sulfonamide) and TQS (4-(1-naphthyl)-3a,4,5,9b-tetrahydro-3*H*-cyclopenta[c]-quinoline-8-sulfonamide) were synthesized as described previously (21, 22). Mecamylamine ((1*S*,2*R*,4*R*)-*N*2,3,3-tetramethylbicyclo[2.2.1]heptan-2-amine) was purchased from Sigma. Fresh acetylcholine (ACh) stock solutions were made each day of experimentation. PNU-120596, TQS, and GAT107 stock solutions were prepared in DMSO, stored at −20 °C, and used for up to 1 month. GAT107, TQS, and PNU-120596 solutions were prepared freshly each day at the desired concentration from the stored stock.

Heterologous Expression of α7 nAChRs in Xenopus Oocytes—The cDNA clones of human α7 nAChR and human resistance-to-cholinesterase 3 (RIC-3) were provided by Dr. Jon Lindstrom (University of Pennsylvania, Philadelphia) and Dr. Millet Treinin (Hebrew University, Jerusalem, Israel), respectively. Mutations at positions 55 and 93 were introduced using the QuikChange site-directed mutagenesis kit (Agilent Technologies, Santa Clara, CA) following the manufacturer's instructions. Mutations were confirmed with automated fluorescent sequencing. Note that the Y93C mutation was made in the Cys-null pseudo-wild-type C116S background (23) to prevent the possible formation of spurious disulfide bonds. Subsequent to linearization and purification of the plasmid cDNAs, cRNAs were prepared using the mMessage mMachine *in vitro* RNA transfection kit (Ambion, Austin, TX).

Oocytes were surgically removed from mature female *Xenopus laevis* frogs (Nasco, Ft. Atkinson, WI) and injected with cRNAs of α7 nAChR and RIC-3 as described previously (24). The RIC-3 chaperone protein can improve and accelerate α7 expression with no effects on the pharmacological properties of the receptors (25). Frogs were maintained in the Animal Care Service facility of the University of Florida, and all procedures were approved by the University of Florida Institutional Animal Care and Use Committee. In brief, the frog was first anesthe-

tized for 15–20 min in 1.5 liters of frog tank water containing 1 g of 3-aminobenzoate methanesulfonate (MS-222) buffered with sodium bicarbonate. The harvested oocytes were treated with 1.4 mg/ml collagenase (Worthington) for 3 h at room temperature in a calcium-free Barth's solution (88 mM NaCl, 1 mM KCl, 2.38 mM $NaHCO_3$, 0.82 mM $MgSO_4$, 15 mM HEPES, and 12 mg/liter tetracycline, pH 7.6) to remove the follicular layer. Stage V oocytes were subsequently isolated and injected with 50 nl of 6 ng of α7 nAChR subunit cRNA and 3 ng of RIC-3 cRNA. Recordings were carried out 1–7 days after injection.

Two-electrode Voltage Clamp Electrophysiology—Experiments were conducted using OpusXpress 6000A (Molecular Devices, Union City, CA) (24). Both the voltage and current electrodes were filled with 3 M KCl. Oocytes were voltage-clamped at −60 mV except when determining the effect of voltage on channel activation. The oocytes were bath-perfused with Ringer's solution (115 mM NaCl, 2.5 mM KCl, 1.8 mM $CaCl_2$, 10 mM HEPES, and 1 μM atropine, pH 7.2) with a flow rate of 2 ml/min. To evaluate the effects of experimental compounds on ACh-evoked responses of α7 nAChRs expressed in oocytes, two initial control responses to applications of ACh were recorded before test applications of experimental drugs alone or co-applied with the ACh. The agonist solutions were applied from a 96-well plate via disposable tips, and the drugs were either co-applied with ACh by the OpusXpress pipette delivery system or bath-applied using the OpusXpress system to switch the running buffer. Drug applications were 12 s followed by a 181-s washout period and usually alternated between control and test solutions. Control concentrations of ACh were 60 μM for wild-type α7 and α7M254L, 100 μM for α7Trp-55 mutants, 300 μM for α7Y93A, and 1 mM for α7Y93G. Because α7Y93C and α7Y93S did not respond to ACh or other orthosteric activators, 3 μM GAT107 was used as a control in some experiments for these receptors. In other experiments with α7Y93C, the data were not normalized but just expressed as absolute magnitude of peak current (μA) or net charge (μA seconds) (26). After experimental drug applications, follow-up control applications of ACh were made to determine primed potentiation, desensitization, or rundown of the receptors.

Data were collected at 50 Hz, filtered at 20 Hz, analyzed by Clampfit 9.2 (Molecular Devices) and Excel (Microsoft, Redmond WA), and normalized to the averaged current of the two initial control responses (26). Data were expressed as means ± S.E. from at least four oocytes for each experiment. Responses were measured as both peak currents and net charge as reported previously (26). Net charge is a more reliable indicator of the concentration dependence of α7 activation by orthosteric agonists and comparisons of effects on peak current, and net charge is the feature that distinguishes type I (ratio of amplification close to 1) and type II PAMs (higher amplification of net charge than of peak current) (19). In most experiments, the normalized effects of drug applications were calculated as the ratio of the experimental response (peak current or net charge, as indicated) to the average of the two control ACh-evoked responses obtained prior to any drug applications. Data were plotted by Kaleidagraph 3.0.2 (Abelbeck Software, Reading, PA), and curves were generated as the best fit of the average values from the Hill equation.

RESULTS

Three Forms of GAT107 Activity—Using our standard protocol of alternating control ACh applications with applications of experimental drugs, we identified three distinct forms of GAT107 (Fig. 1*A*) effects on the currents of *Xenopus* oocytes expressing human α7 nAChR (Fig. 1). We observed, as expected (20), significant transient activation of the α7 ion channels during the direct application of GAT107 (Fig. 1*B*). These currents were much larger than control responses to ACh and decayed to baseline as GAT107 was washed out of the bath. The second form of GAT107 activity observed was the expected direct potentiation obtained when GAT107 and ACh were co-applied (Fig. 1*C*). The third form of GAT107 activity we term "primed potentiation." This mode involves potentiation of agonist-evoked responses after GAT107 has been applied, with an intervening washout period prior to the agonist (*e.g.* ACh) application. This is evident in the ACh control responses after the GAT107 direct activation (Fig. 1*B*) or primed potentiation (Fig. 1*C*). This prolonged aftereffect of GAT107 has not previously been characterized in detail and shows that the drug is working on two different time scales because the primed potentiation is observed after the direct activation has been terminated by drug washout and, unlike direct potentiation, requires only the application of the orthosteric agonist.

Concentration-response studies of the direct activation of α7 by 12-s applications of GAT107 indicated that GAT107-evoked peak currents and net charge values were 38 ± 8-fold and 514 ± 28-fold (Fig. 1*D*), larger than initial control responses to ACh, respectively. The data were not well fit by the Hill equation. Maximal peak currents and net charge were obtained at concentrations of 30 and 100 μM, respectively (Table 1, Direct activation). As noted above, direct activation was only observed as long as drug was in the bath solution, presumably without requiring any added orthosteric ligand.

The first crystal structures of the molluscan acetylcholine-binding protein, a pentameric protein that has been the basis for structural models of the α7 extracellular domains, had molecules of the buffer HEPES in the orthosteric binding site (27). Because the normal Ringer's recording solutions are HEPES-buffered, we also conducted some experiments (data not shown) in HEPES-free (phosphate/bicarbonate-buffered) Hanks' balanced salt solution. These experiments confirmed that the direct activation of α7 by GAT107 did not depend on HEPES acting as a surrogate orthosteric ligand. Likewise, direct activation produced by 10 μM GAT107 did not require the prior control applications of ACh in our usual protocol. Cells ($n = 6$) that were treated with GAT107 without previous ACh had peak currents of 12.4 ± 1.5 μA, whereas cells from the same injection set recorded on the same day had peak currents in response to 10 μM GAT107 of 11.1 ± 1.7 μA after two previous control applications of 60 μM ACh. Note that the standard errors for the responses evoked by GAT107 are relatively large, as would be expected. We have previously published (3, 28) that the effect of an efficacious PAM such as PNU-120596 is to increase the activity of a very small percentage of the channels (1–2%) by a very large factor (200,000-fold). The stochastic nature of such

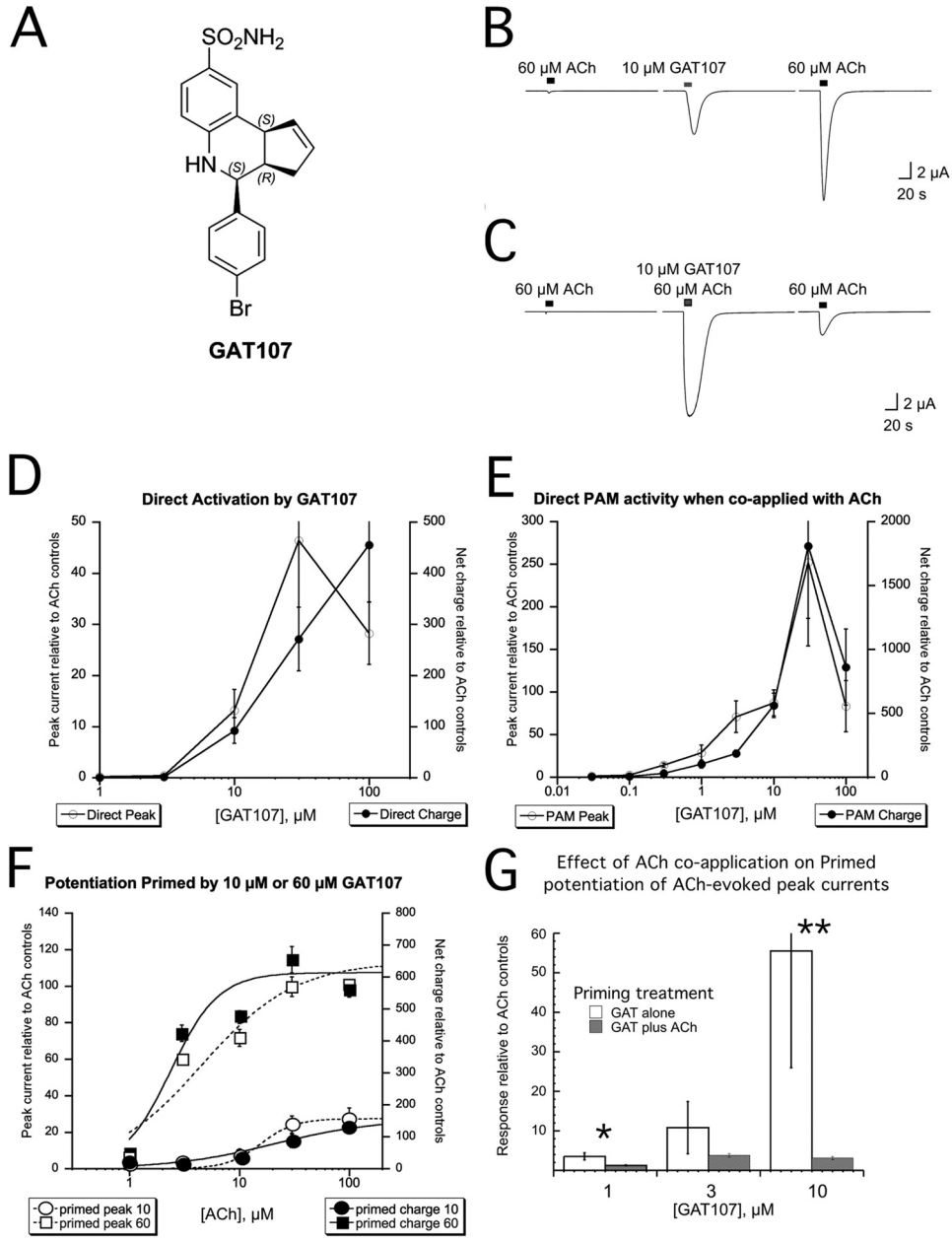

FIGURE 1. **GAT107 and three phases of its activity on human α7 nAChR expressed in *Xenopus* oocytes.** *A,* structure of GAT107. *B,* representative data illustrating a control response of human α7 nAChR to a 12-s application of 60 μM ACh followed by 10 μM GAT107 and then 60 μM ACh again. Note that the application of GAT107 alone produces a robust transient "direct response" and that there is a residual effect that produces primed potentiation. *C,* representative data illustrating a control response of human α7 nAChR to a 12-s application of 60 μM ACh followed by the co-application of 10 μM GAT107 plus 60 μM ACh and then 60 μM ACh alone. The large response from the co-application is direct potentiation. Primed potentiation is the increased response to ACh following the application of GAT107 applied alone or with ACh. Note that primed potentiation is greater after direct activation (*B*) than after direct potentiation (*C*). Note that traces in *A* and *B* are scaled relative to their initial ACh controls. *D,* concentration-response data for direct activation by GAT107 applied alone. *E,* concentration-response data for direct potentiation by GAT107 co-applied with 60 μM ACh. *F,* concentration-response data for primed potentiation of ACh-evoked responses by prior application of either 10 μM (*circles*) or 60 μM GAT107 (*squares*) applied alone. *D–F,* the peak currents (*open symbols, left scale*) and net charge (*filled symbols, right scale*) of the GAT107-evoked responses are compared with the respective measurements from the average of two control 60 μM ACh-evoked responses obtained from the same cells prior to the application of GAT107 applied alone (*D* and *F*) or in combination with ACh (*E*). Each point is the average of at least four cells (±S.E.). See Table 1 for summary data. *G,* effect of ACh co-application with GAT107 on the primed potentiation of subsequent responses to ACh applied alone. *, $p < 0.05$. Responses following the application 10 μM GAT107 alone were significantly higher (**, $p < 0.01$) than those following the co-application of GAT107 and ACh (see *B* and *C*).

effects will naturally produce large variances in the macroscopic responses, because a small change in the number of open channels will produce large changes in the size of a summated response.

Concentration-response studies of the direct potentiating effects of varying concentrations of GAT107 co-applied with a fixed concentration of 60 μM ACh are shown in Fig. 1*E*. The maximal peak currents and net charge values of responses evoked by these co-applications were 3–5-fold larger than those evoked by the direct activation with GAT107 alone (Table 1, Direct potentiation). The data were not described by the Hill equation because responses to co-applications of ACh

TABLE 1
Efficacy and potency of GAT107 effects

Direct activation by GAT107†

Peak current		Net charge	
I_{max}	[GAT107]*	I_{max}	[GAT107]
46 ± 19	30 μM	455 ± 111	100 μM

Direct potentiation by GAT107

Peak current		Net charge	
I_{max}	[GAT107]	I_{max}	[GAT107]
252 ± 89	30 μM	1807 ± 563	30 μM

Primed potentiation of ACh responses following GAT107 applied alone, effects on ACh potency and efficacy

[GAT107]	Peak current		Net charge	
	I_{max}	EC_{50}	I_{max}	EC_{50}
10 μM	27 ± 1.5	16 ± 2	154 ± 8	20 ± 3
60 μM	113 ± 14	4.5 ± 2.2	614 ± 44	2.4 ± 0.6

† I_{max} values are fold-increases over 60 μM ACh-evoked control responses.
* Note that the concentration-response data for direct GAT107 activation and potentiation of responses evoked by co-application with 60 μM ACh were not suitable for fit by the Hill equation, and the I_{max} values reported are those empirically measured at the indicated concentrations.

with 100 μM GAT107 were less than those with 30 μM GAT107. This is consistent with previous studies of the PAM PNU-120596 (3), which indicated that high concentrations of a PAM can preferentially induce a PAM-insensitive form of desensitization.

The primed potentiation of ACh-evoked responses produced by prior application of GAT107 was dependent on both the GAT107 concentration used for priming and the concentration of ACh subsequently applied (Fig. 1*F*). Priming with the higher concentration of GAT107 not only produced larger responses but also increased the apparent potency of ACh (Table 1, Primed potentiation). Although primed potentiation could be produced by either prior direct activation (Fig. 1*B*) or direct potentiation (Fig. 1*C*), it was less when it followed the stronger stimulation of direct potentiation (Fig. 1*G*). This is also consistent with strong activation producing a form of PAM-resistant desensitization (D_i), previously described for PNU-120596 (3).

There are two fundamental modes for the positive allosteric modulation of α7 nAChR (12). One mode, barrier modulation, affects the energy barriers between conducting and nonconducting states but not the absolute free energy of the states. This mode will operate on a population of receptors responding synchronously to agonist application and will produce a transient increase in channel opening. PAMs, which are classified as type I (19), appear to operate strictly in this mode. The other mode is equilibrium modulation, which affects the relative stability of conducting and nonconducting (*i.e.* desensitized) states. Equilibrium modulation will produce protracted increases in current and may reverse some forms of desensitization (D_s states) promoted by agonist binding, although other nonconducting states (D_i states) may remain insensitive to the effects of the PAM. Like PNU-120596, GAT107 has both barrier and equilibrium modulation effects, which are apparent when the drug is bath-applied for a prolonged period of time. However, as shown in Fig. 2, the kinetics of direct activation by application of GAT107 alone are relatively slow when the drug is at low concentration, consistent with the effects being largely on the conformational equilibrium among conducting and nonconducting states. When ACh was added to the bath applications along with GAT107, there was a shift in the pattern of activation, with a large but transient initial phase of activation that decayed to a protracted steady-state balance between activating and desensitized channels. With strong initial phases of activation, the steady-state currents were less, and upon washout there appeared to be relaxation of some of the equilibrium desensitization. Similar currents with large initial transient responses decaying to a low steady state were observed when ACh was bath-applied following a single priming application of GAT107 (Fig. 2*B*). There was no pronounced effect of the ACh concentration when bath applications of 60 or 300 μM were made on either phase of the responses, and there were no significant differences in the accumulated net charge values. Note, however, that the brief 2-min washout was sufficient to resensitize the receptors for another large current due to primed potentiation.

The direct activation previously reported for racemic 4BP-TQS was hypothesized to be due solely to binding at the same site (20) as for allosteric modulation. However, it is unclear if this is the case because the direct activating effects are only manifested when GAT107 is in the external solution, although the PAM effects persist long after the free drug is washed away. It was previously reported that the direct activation produced by 4BP-TQS was sensitive to methyllycaconitine (MLA). We confirmed that was also true for the direct activation produced by GAT107 (Fig. 3, *A* and *B*). Although MLA is considered to be a competitive antagonist of orthosteric agonists, as reported previously (20), we found that the inhibition of GAT107 direct activation was not surmountable by increasing concentrations of GAT107 (data not shown). This is consistent with MLA acting as a sort of an inverse agonist, as we have previously seen when it was applied to receptors with tethered agonists (29). Although this effect of MLA is consistent with GAT107 not producing direct activation by binding to the orthosteric site, it is not sufficient to prove that GAT107 is working exclusively at a single allosteric site to produce both potentiation and direct activation. In fact, co-applications of MLA with GAT107 suppressed direct activation, and MLA had no significant effect on the primed potentiation (Fig. 3*C*). The differences in reversibility and MLA sensitivity indicate clear differences in the GAT107 mode and site of action for direct activation and primed potentiation.

There are several lines of evidence that indicate that the state of the receptor in the ion conduction pathway is different when conducting ions following PAM potentiation, compared with when it is conducting ions following activation at the orthosteric site alone. For example, channels activated by ACh alone or ACh and PNU-120596 differ in their sensitivity to noncompetitive antagonists (30). Additionally, it has been shown that PNU-120596-potentiated ion currents do not show the inward rectification that characterizes α7 currents under control conditions (30, 31). Consistent with these observations, our data indicated that currents directly activated by GAT107 were also large when the cells are held at +50 mV (data not shown), and the application of GAT107 at +50 mV was effective at producing primed potentiation. Likewise, when direct activa-

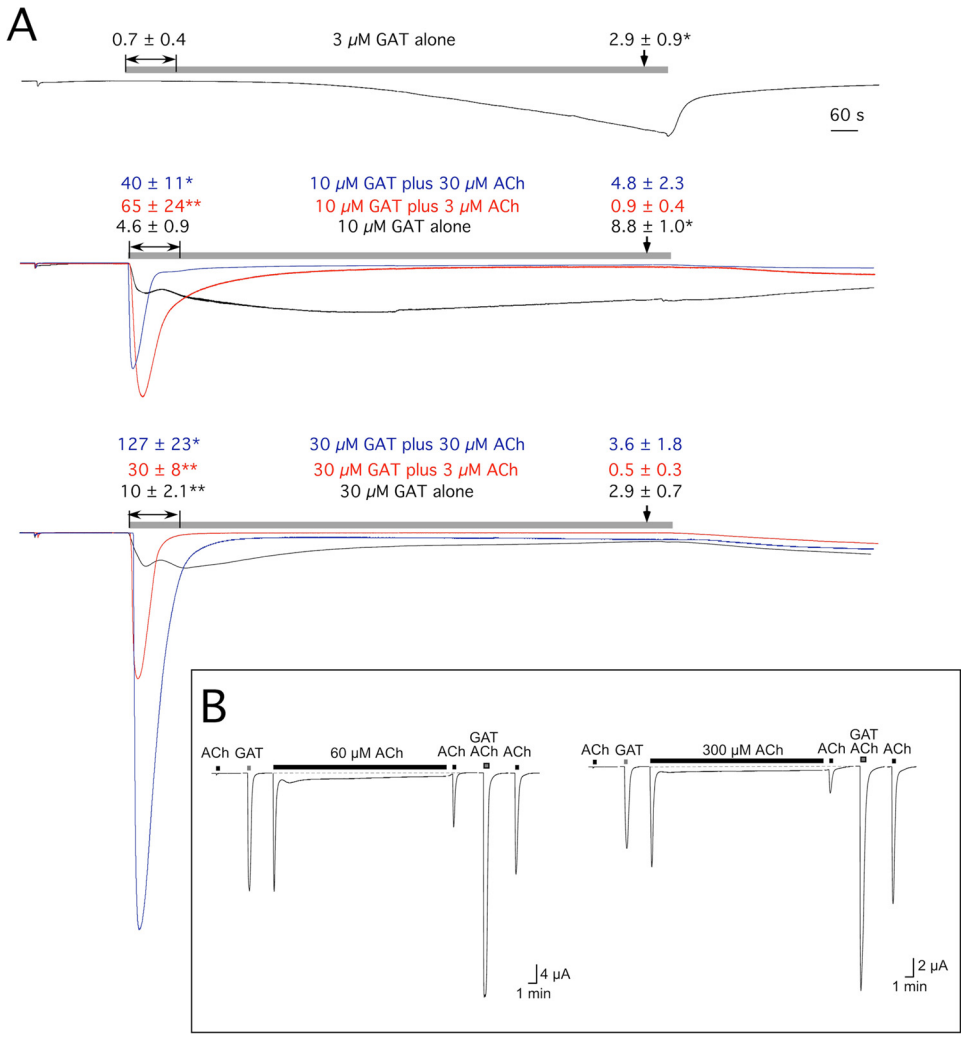

FIGURE 2. *A,* concentration and time dependence of direct activation and direct potentiation of human α7 expressed in oocytes by GAT107. Representative traces of responses were obtained when varying concentrations of GAT107 (*GAT*) were bath-applied for 20 min with or without ACh at the indicated concentrations. All traces are scaled relative to their initial ACh controls. The values *above* the traces are the peak current amplitudes recorded in the first 120 s (*left*) or the offset from baseline recorded at 60 s prior to the end of the bath application (*right*). The units are fold-increases relative to the average peak currents of two control 60 μM ACh-evoked responses obtained from the same cells prior to the bath applications. Values are the average of at least four cells (± S.E.). *t* tests were conducted to determine whether amplitude of the initial peaks were significantly different from the baseline offset at the end of the application (*, $p < 0.05$; **, $p < 0.01$). *B,* primed potentiation of ACh-evoked currents with prolonged (20 min) bath applications of ACh following a single application of 10 μM GAT107 (*GAT*). *Traces* are scaled relative to their initial ACh controls. There was no significant difference in the net charge ($n = 4$) of the responses to the bath application of 60 or 300 μM ACh. After 20 min there appeared to be a large amount of equilibrium desensitization that reversed after a brief wash.

tion was generated at −60 mV and then the primed potentiation was tested at +50 mV, the GAT107 potentiated currents showed similar relief of inward rectification as reported for PNU-120596 potentiated currents (data not shown).

We characterized the duration of the potentiation primed by GAT107 and the effects of ACh co-applications on decreasing that activity. We investigated the stability and duration of primed potentiation by making single applications of 10 or 60 μM GAT107 followed by eight ACh applications at 4-min intervals (Fig. 4*A*). The priming effects of a single GAT107 application appeared relatively long lasting, suggesting either very slowly reversing binding to the allosteric site or the induction of a very stable conformational state. Following a single application of 10 μM GAT107, ACh-evoked net charge responses became stable after the second ACh application at levels ~150-fold greater than the ACh controls, with no decrease up to 32 min. When the priming application of 10 μM GAT107 was paired with 60 μM ACh, the primed potentiation was less, as expected, and remained stable at 50–60-fold over the ACh controls for the full 32 min. When 60 μM GAT107 was used for priming, the magnitude of the potentiation was greater and the effect of pairing the GAT107 with ACh was less. After 32 min, the ACh-evoked responses were 297 ± 80 and 243 ± 26 times greater than the initial ACh controls for cells receiving GAT107 alone or in combination with ACh, respectively.

We have previously reported that the potentiating effects of PNU-120596 are also relatively long lived. In Fig. 4*B,* we compare the aftereffects of a single application of 10 μM GAT107 to those produced by a single application of either 30 μM PNU-120596 or TQS. There was similar persistence of the primed potentiation for all three agents; however, the magnitude of the potentiation differed. Although the GAT107-primed potentiation was stable at about a 150-fold increase over the initial ACh controls, the TQS net charge-primed potentiation was approx-

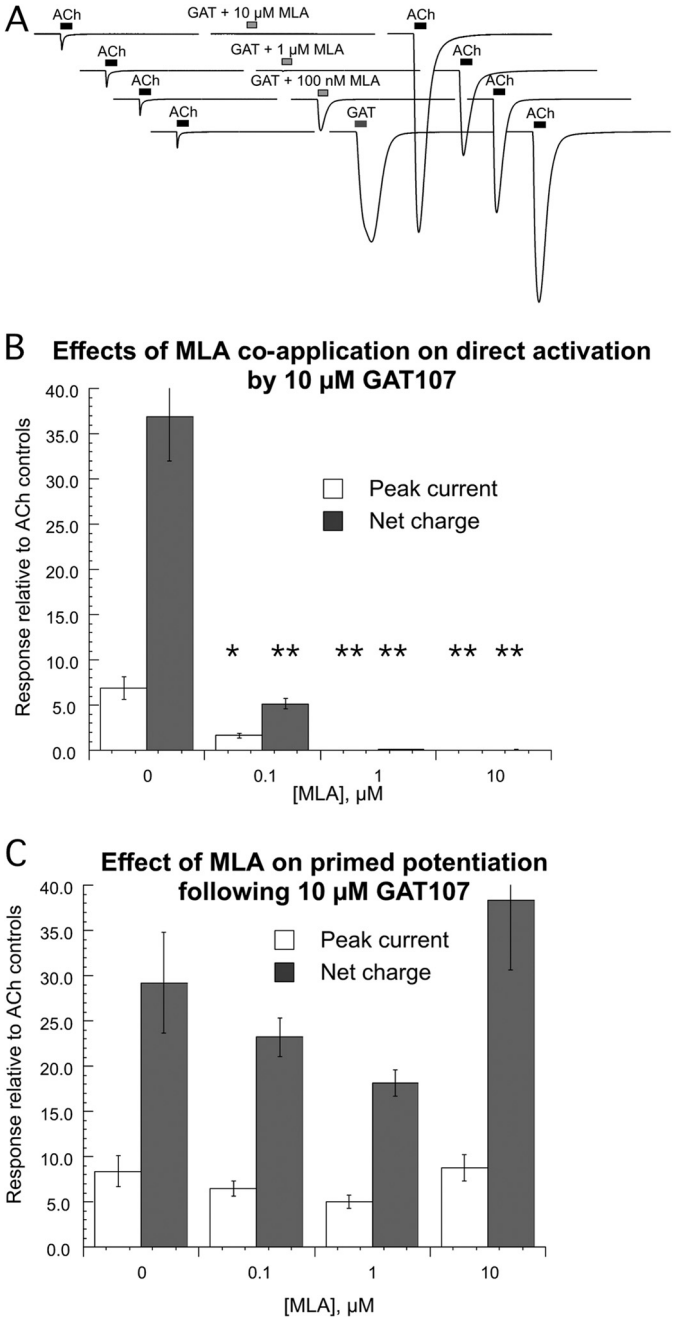

FIGURE 3. *A,* sample traces illustrating effects of MLA co-application on the direct activation and primed potentiation produced by 10 μM GAT107 on human α7 expressed in oocytes. *B,* average data on the effect on MLA on the responses directly activated by co-application with 10 μM GAT107. *C,* average data on the effect on MLA on ACh-evoked responses following the application with 10 μM GAT107 with or without MLA. *B* and *C,* each *bar* represents the average net charge response of at least four cells (± S.E.) relative to the average of two initial ACh control responses from the same cells. The post GAT107 ACh applications were 60 μM at the standard 4-min interval, as in *A*. *Asterisks* indicate conditions where MLA significantly reduced currents relative to those obtained in the absence of MLA (*, $p < 0.05$; **, $p < 0.01$).

imately a 45–50-fold increase, and the PNU-120596-primed potentiation was only a 2–3-fold increase.

Repeated applications of GAT107 to cells expressing α7 produced direct activation responses of relatively stable magnitude. To determine whether primed potentiation accumulated during these repeated applications, we compared ACh responses after three 10 μM GAT107 applications to one 10 μM GAT107 application followed by two applications of Ringer's solution or 60 μM ACh. As shown in Fig. 4*C*, the primed potentiation of the ACh application was significantly greater ($p < 0.05$) after three applications of GAT107 than with the other protocols.

Hypothesis of Multiple Modes and Multiple Binding Sites—To provide a framework for the interpretation of GAT107's effects on wild-type receptors and a context for an analysis of α7 mutants, hypothetical models for the three forms of GAT107 activity (summarized in Table 2) are presented in Fig. 5. Although the location of the binding site for orthosteric agonists (A) has been well characterized, the binding site(s) for PAMs (P) are less well characterized but probably located in the transmembrane domains (13). Our data suggest the site associated with the direct activation produced by GAT107 (G) is likely to be distinct from the PAM site, because the activity associated with this site differs from the PAM activity in being rapidly reversible (on the time scale of solution washout) and MLA-sensitive. We hypothesize that this distinct site might be located in the region of the interface between the extracellular and transmembrane domains, because studies of chimeric receptors implicated this as a domain of secondary significance for allosteric modulation (32). This location is also supported by preliminary docking studies of GAT107 into an α7 homology model (data not shown). We show in Fig. 5*B* the hypothetical free energy landscapes, as described previously for ACh and PNU-120596 (3), that might be associated with receptors with ligands bound to the orthosteric, allosteric, and direct activation sites. Because GAT107 appears to dissociate rapidly from the direct activation site but slowly from the PAM site, we represent these sites in Fig. 5*B* as a *hexagon* and a *triangle,* respectively, to suggest greater complementarity between the ligand (also represented as a *triangle*) and the PAM site.

As we have hypothesized for ACh and PNU-120596 (3), the free energy landscapes will vary as a function of the fractional occupancy of the multiple sites on the five α7 subunits. For the purpose of this illustration, we have selected landscapes that would correspond to the level of occupancy most likely to promote activation, based on previous studies of fractional occupancy of ACh and PNU-120596 (3). Note that we omit one feasible configuration of site occupancy, that of "G" only. This configuration could exist only briefly at the beginning of an application of GAT107 alone. Therefore, it is likely that the currents generated during direct activation arise from binding at both the G and "P" sites. This is consistent with the observation that the M254L mutation, which strongly limits the direct potentiation effects of both PNU-120596 and 4BP-TQS (13, 20), also limits the direct activation by GAT107 (data not shown).

The hypothetical free-energy landscapes in Fig. 5*B* can be viewed in two different ways as follows: changes in energy barriers for conformational transitions or relative equilibrium energy of the states. The perspective provided by the energy barriers is most relevant to the nonstationary conditions that follow from an abrupt change in ligand concentration, which initially affects a population of receptors in synchrony, generating a large transient activation that subsequently decays

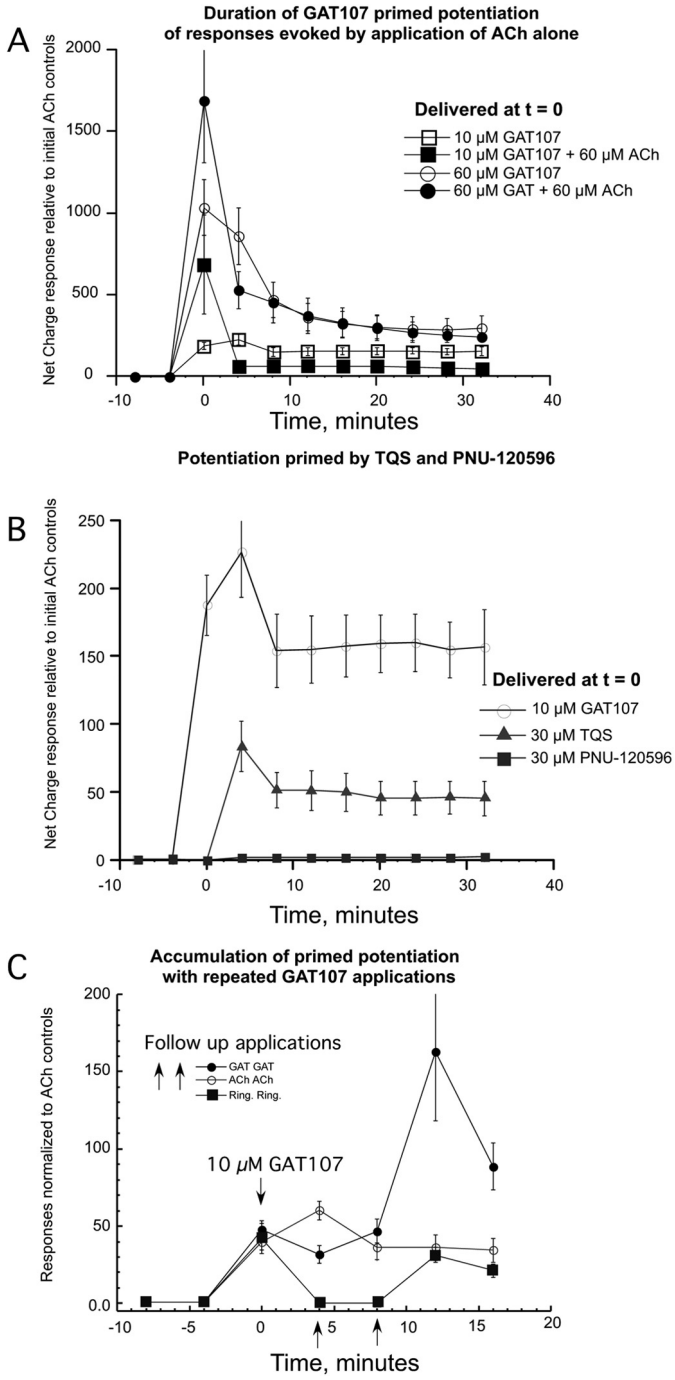

FIGURE 4. *A,* persistence of primed potentiation of net charge responses to repeated applications of 60 μM ACh produced by single applications of either 10 or 60 μM GAT107 applied alone or co-applied with 60 μM ACh on human α7 expressed in oocytes. Co-applications produced greater initial responses but less primed potentiation. Each point represents the average net charge response of at least four cells (±S.E.) relative to the average of two initial ACh control responses from the same cells. *B,* persistence of primed potentiation of net charge responses to repeated applications of 60 μM ACh produced by single applications of 30 μM PNU-120596 or TQS compared with the data for 10 μM GAT107 applied alone from *A*. Co-applications produced greater initial responses but less primed potentiation. Note that the primed potentiated responses were relatively stable for 30 min. Each point represents the average net charge response of at least four cells (± S.E.) relative to the average of two initial ACh control responses from the same cells. *C,* accumulation of primed potentiation. To determine whether repeated applications of GAT107 produce more primed potentiation than single applications, even though the direct responses to GAT107 do not increase with repetition, cells were given an application of 10 μM GAT107 and two follow-up applications of 10 μM GAT107, 60 μM ACh, or Ringer's solution. Although the primed potentiation measured as net charge at 12 min was the same for cells receiving ACh or Ringer's follow-up, it was significantly larger ($p < 0.05$) for cells receiving GAT107 follow-ups. Each point represents the average net charge response of at least four cells (±S.E.) relative to the average of two initial ACh control responses from the same cells.

TABLE 2
Three forms of GAT107 activity on wild-type α7 nAChR

Direct activation
Activation independent of orthosteric agonists
Requires GAT107 freely diffusible in solution
Reverses rapidly upon washout
Blocked by co-application with MLA
Hypothesized to require binding to a unique site
Primed potentiation
Activation requires pre-application of GAT107, followed by orthosteric agonist alone
Requires agonist in solution but persists after GAT107 is washed out
Is induced by GAT107 application in the presence of MLA
Is reduced following strong activation of GAT107 co-applied with agonist
Direct potentiation
Requires co-application of GAT107 and orthosteric agonist
Associated with large transient and variable steady-state currents
Kinetics depend on agonist and GAT107 concentrations
Inverted "U" concentration- response function

toward an equilibrium distribution of receptors among the states (see Fig. 2). In terms of the raw data measured in voltage clamping, this corresponds to peak height. This process is illustrated in Fig. 5*C* for a population of receptors (represented by the *red circle*) that are in the resting state prior to a rapid application of ACh and GAT107. The progression of the receptors through the conformational landscape will be initially influenced exclusively by the energy barriers for transitions out of the resting state, but after the receptors equilibrate among the states, they will approach a distribution associated with their relative energy levels, qualitatively related to net charge and ultimately to steady-state current.

Structural Basis for Activation Coupling between Orthosteric and Allosteric Binding Sites—Previous studies of site-directed mutants have identified critical residues for the functioning of the orthosteric and allosteric binding sites of α7 nAChR. The orthosteric binding site has been extensively mapped (33), and critical residues like Tyr-188 and Trp-149 were identified (34–37). Likewise, amino acid Met-254 in the transmembrane domain has been identified to be essential for the function of allosteric potentiators, whereas mutations in the second transmembrane domain, such as L248T (L9′T), have effects on their own that are similar to those of allosteric potentiators. However, it remains an open question how the activity of these two domains are coupled so that the potentiating effects of agents such as PNU-120596 and TQS also require the effects of orthosteric agonists, or how orthosteric agents modify the effects of the ago-PAM GAT107 for both direct and primed potentiation. An attractive target domain in which to look for residues that might mediate such coupling is the interface between subunits on the periphery of the orthosteric binding site. One residue in this domain, Trp-55, has previously been implicated for determining the efficacy and selectivity of specific orthosteric ligands in both α7 and heteromeric receptors such as those containing α4 and β2 subunits (35, 38).

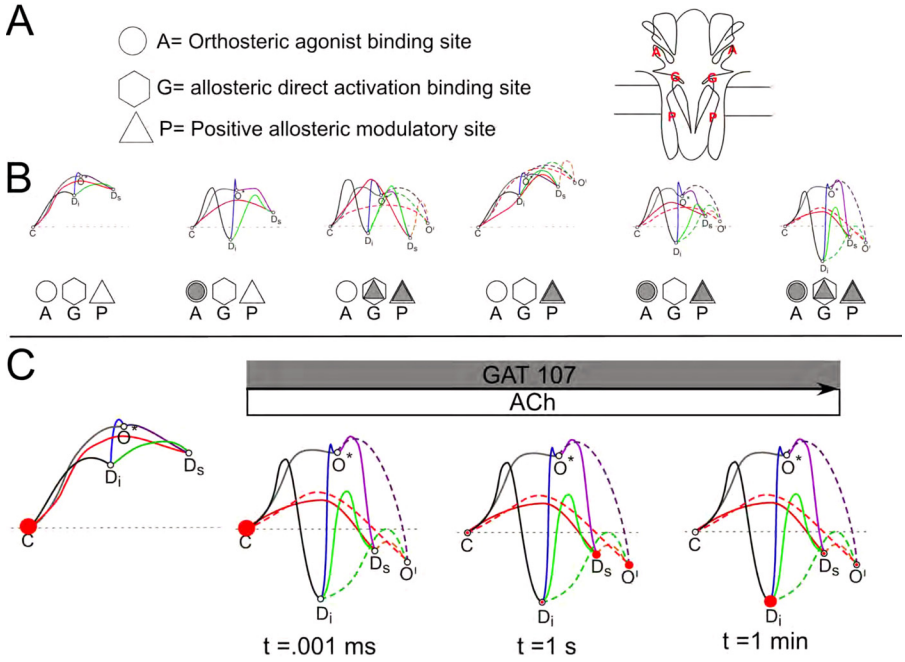

FIGURE 5. *A,* postulated multiple binding sites controlling the activation and desensitization of α7 nAChR. *B,* different possible configurations of site occupancy by an orthosteric agonist such as ACh (represented by the *filled circle*) or the allosteric ligand GAT107 (represented by the *filled triangle*). Each of the five subunits would contain all three of these postulated sites and, depending on the ligands available, could have any one of the occupancy patterns indicated. Note that one additional configuration might occur, with only the G site occupied, but this would exist only briefly and may not be functionally important, so it is not indicated. The conformational landscapes illustrated in *B* can be used to visualize the dynamic character of the responses as the population reacts to rapid change in ligand concentrations, derived from previously published models (3). The schematics are based on rate theory and visually convey information equivalent to Markov models. The humps represent energy barriers between states, so that the heights of the barriers are proportionate to the logs of the rate constants in a Markov model, and the positions of the states represent the relative free energy (stability) of the states. There is no intrinsic significance to the colors of the lines; they are colored only to make it easier to follow them from one state to another. The *dotted lines* connect the novel conduction state of the potentiated receptors to the states that are associated with the control condition. With the co-application of ACh and GAT107, the receptors would shift rapidly from the resting condition with all the sites unbound to the resting condition with A, G, and P sites occupied. *C,* use of the energy landscapes to predict the behavior of receptors after a rapid application of ACh and a PAM. The occupancy of specific conformational states as a function of time is represented by the size of the *red circles* in the diagrams. Over time, occupancy of the A, G, and P sites will shift the distribution of receptors in the conformational states toward the one that is most stable (*i.e.* the D_i state).

GAT107 is a very effective direct activator of the W55A α7 mutant (Fig. 6*A*), to such a degree that co-application of GAT107 with ACh did not significantly increase responses compared with GAT107 alone. This effect was observed across ranges of GAT107 and ACh concentrations (Fig. 6*B*) and appeared to be due to fundamentally larger direct activation responses compared with wild type (Fig. 6*C*). Similar results were obtained with other α7Trp-55 mutants (Table 3) and with alternative orthosteric agonists on W55A (data not shown).

The enhanced activity of GAT107 when applied alone to α7W55A was not consistent with the direct activation of wild-type α7 in several important regards. Although direct activation of wild-type α7 persisted only as long as GAT107 was freely diffusible in the bath (Fig. 7*A*), the activations of α7W55A were more persistent, and residual activation accumulated with repeated or prolonged applications (Fig. 7*A*). The response to a prolonged bath application of GAT107 to α7W55A-expressing cells also produced a distinctly more biphasic or even triphasic response, resembling, to some degree, the responses of wild-type α7 to ACh plus GAT107, except with a much larger steady-state component (Fig. 7*B*). Additionally, although the direct activation of wild-type α7 by GAT107 was MLA-sensitive (Fig. 3), responses of α7W55A to 10 μM GAT107 were insensitive to co-application of 1 μM MLA (Fig. 8*A*). Note that, in addition to producing prolonged activation of α7W55A, GAT107 could still produce primed potentiation of this mutant (Fig. 8*B*), although the effect was not as large as with wild-type α7 and was suppressed following prolonged GAT107 application (Fig. 7*B*).

These data suggested that the activating properties of GAT107 working at the potentiation site were decoupled from the augmenting effects of ligands at the orthosteric site, and so we tested the effect of the PAMs TQS and PNU-120596 on α7W55A mutant receptors. As shown in Fig. 9*A*, both of these agents were able to directly activate α7W55A in a manner more consistent with protracted PAM-like activity than the transient direct activation of wild-type α7 by GAT107. To determine the extent to which these PAMs were decoupled from the orthosteric binding site in α7W55A, we tested them alone or co-applied with 60 μM ACh. As shown in Fig. 9*B*, responses to 3 and 10 μM TQS were increased when combined with ACh, but the responses to 30 μM TQS were not increased by co-application with ACh. In contrast, at all concentrations of PNU-120596 tested, responses were larger when the PAM was co-applied with ACh (Fig. 9*C*) than when PNU-120596 was applied alone.

Trp-55 is situated on the complementary surface of the orthosteric binding site. We wished to determine whether proximal residues on the primary (α-like) side of the subunit interface might have independent or complementary roles in coupling orthosteric and allosteric activation. In the homology model of the α7 receptor derived from the acetylcholine-bind-

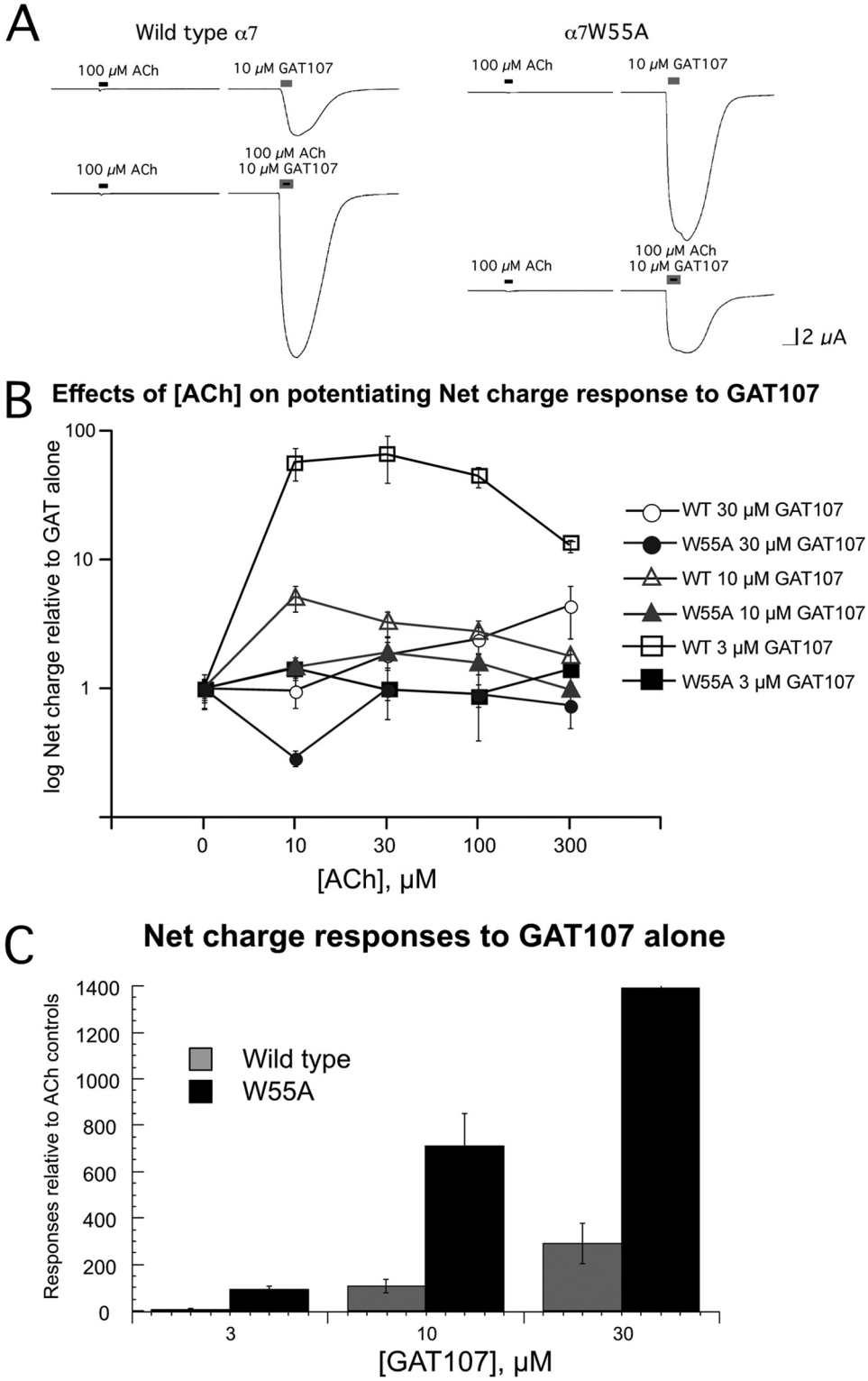

FIGURE 6. *A,* representative data illustrating the effect of the W55A mutation on the relative magnitude of GAT107 direct activation and direct potentiation compared with controls. *B,* interaction between GAT107 and ACh for producing direct potentiation of wild-type α7 and α7W55A nAChR, expressed relative to the net charge of a direct activation response (0 ACh). Each *point* represents the average net charge response of at least four cells (±S.E.) relative to the average of two initial ACh control responses from the same cells. Note that the *y* scale is in log units. *C,* direct activation (net charge) of wild-type α7 and α7W55A receptors by three different concentrations of GAT107.

ing protein crystal structure, Tyr-93 is positioned just across the subunit interface from Trp-55 (Fig. 10). We have previously reported (23) that a cysteine mutation placed at this site (in a C116S Cys-null pseudo-wild-type α7) failed to yield receptors that gave functional responses to ACh. From those data, it was unclear whether α7Y93C formed receptors that were not functional in regard to orthosteric activation or whether the receptors failed to traffic in functional form to the cell membrane. To

evaluate this, cells were injected with RNA for wild-type α7 and various Trp-55 or Tyr-93 mutants, as well as a W55Y,Y93W double mutant. After 3 days to allow for expression, the cells were all tested for responses to 100 μM ACh or 10 μM GAT107. Although the receptors varied greatly in their responses to ACh, they all responded well to the application of GAT107 (Fig. 11). Note that although cells expressing Y93C gave no detectable responses to ACh, as expected, cells expressing Y93A had small but clearly detectable ACh responses. We subsequently determined that the size of the Y93A ACh-evoked responses to 100 μM ACh was in part due to a reduction in ACh potency for this mutant. The ACh EC_{50} for Y93A was determined to be 300 μM (data not shown), compared with 30 μM for the wild-type (26), so for

TABLE 3
Net charge responses of wild-type and Trp-55 mutants to GAT107 ± ACh

	10 μM GAT107	10 μM GAT107 + 60 μM ACh
WT	127 ± 15	332 ± 51
W55A	920 ± 188	1470 ± 286
W55V	1470 ± 387	1280 ± 144
W55Y	611 ± 146	855 ± 153
W55F	388 ± 60	613 ± 114

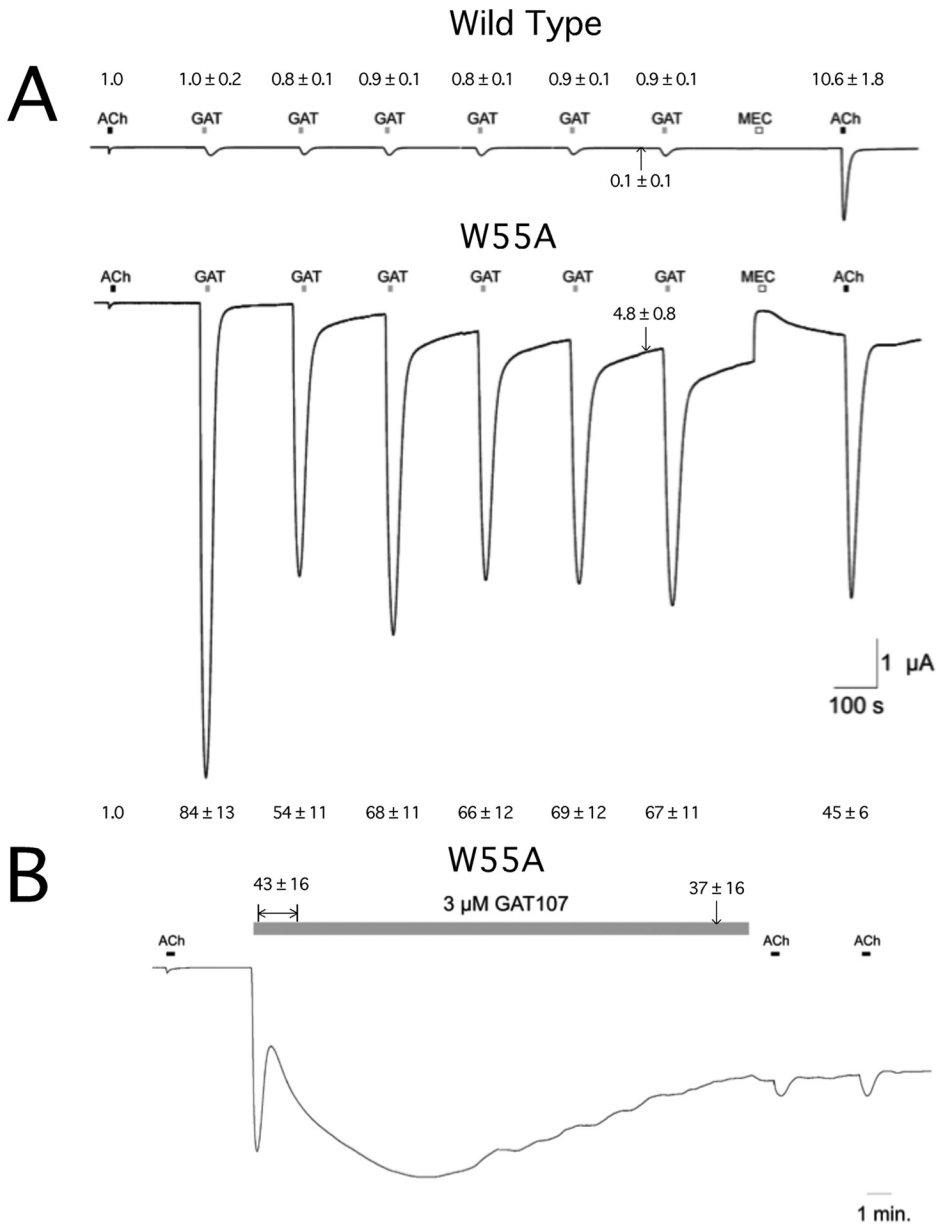

FIGURE 7. **Persistence of GAT107 direct activation of α7W55A nAChR.** *A,* although repeated applications of 3 μM GAT107 (*GAT*) to wild-type α7 receptors produced only a series of small transient responses, a similar series of applications to cells expressing α7W55A produced a progressive build-up of steady-state current that could be inhibited by an application of 100 μM mecamylamine (*MEC*). The values above (*wild type*) or below (*W55A*) the traces are the average peak current amplitudes of at least four cells (± S.E.) for each of the GAT107 applications, measured relative to the initial baseline. The units are fold-increases relative to the average peak currents of two control 60 μM ACh-evoked responses obtained from the same cells prior to the bath applications. Also shown are the average baseline offsets measured at the indicated points. *B,* representative trace illustrating the transient and sustained currents activated by a bath application of 3 μM GAT107 to cells expressing α7W55A (compare with the 1st trace in Fig. 2). The value *above* the traces is the peak current amplitudes recorded in the first 120 s (*left*) or the offset baseline recorded at the indicated time point. The units are fold-increases relative to the average peak currents of two control 60 μM ACh-evoked responses obtained from the same cells prior to the bath applications. Values are the average of at least four cells (± S.E.).

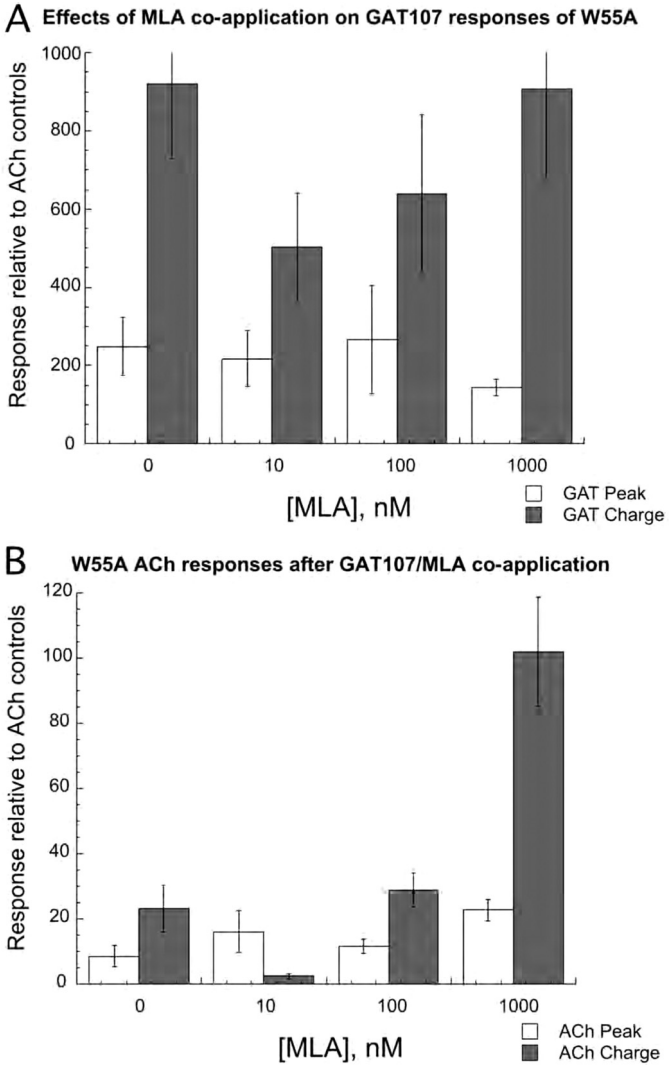

FIGURE 8. **Effects of MLA co-application on the direct activation (*A*) and primed potentiation (*B*) of α7W55A nAChR produced by 10 μM GAT107.** Each *bar* represents the average net charge response of at least four cells (± S.E.), relative to the average of two initial ACh control responses from the same cells. There were no statistically significant effects of MLA.

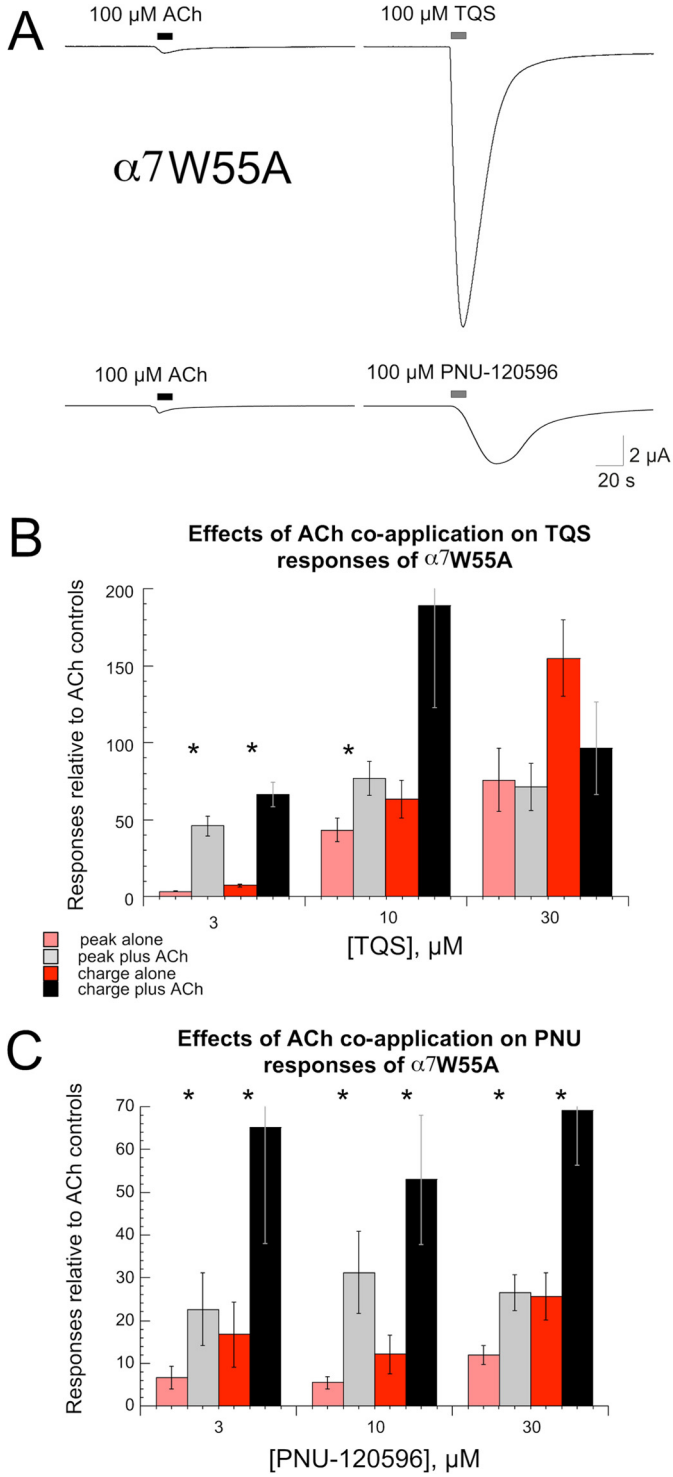

FIGURE 9. **Direct activation of α7W55A by allosteric modulators of wild-type α7 nAChR.** *A,* sample traces of α7W55A responses to TQS and PNU-120596 applied alone. *B,* responses of cells expressing α7W55A to varying concentrations of TQS applied alone or with 60 μM ACh. Note that including ACh produced significant increases in the responses evoked by the two lower concentrations of TQS but not the 30 μM TQS responses. Each *bar* represents the average net charge response of at least four cells (±S.E.) relative to the average of two initial ACh control responses from the same cells. *C,* responses of cells expressing α7W55A to varying concentrations of PNU-120596 applied alone or with 60 μM ACh. Including ACh produced significant increases in the responses evoked by all concentrations of PNU-120596 tested ($p < 0.05$). Each *bar* represents the average net charge response of at least four cells (±S.E.) relative to the average of two initial ACh control responses from the same cells. $p < 0.05$.

subsequent experiments with Y93A mutants, we normalized data to 300 μM ACh control responses.

We tested cells expressing the Y93C mutant with an array of orthosteric agonists, as shown in Fig. 12. Although we failed to detect significant responses to any of the orthosteric agonists, cells responded well to application of GAT107. Responses of cells from the same injection set were smaller ($p < 0.01$) when GAT107 was co-applied with 100 μM ACh (Fig. 12*A*). Cells expressing α7Y93C did not respond to PNU-120596 (data not shown) but did respond to TQS (Fig. 12*B*), albeit at a 10-fold lower level than to GAT107 (Fig. 12*C*). Direct activation of α7Y93C receptors by GAT107 was insensitive to 1 μM MLA (Fig. 12*D*) and was robust when cells were clamped at +50 mV (data not shown). α7Y93A also responded well to GAT107, TQS, and PNU-120596 applied alone, and these responses were likewise observed at positive holding potentials and were insensitive to 1 μM MLA (data not shown).

Consistent with our results obtained with the Y93A mutant, cells expressing a Y93G mutant showed small but detectable

responses to ACh alone at the high concentration of 1 mM. Cells expressing a Y93S mutant showed no detectable response to 1 mM ACh. However, despite their relative insensitivity to ACh alone, both the α7Y93A and α7Y93S receptors could be directly activated by GAT107 alone and showed both primed and direct potentiation of ACh responses (data not shown).

Note that although the ACh responses of the small residue substitutions (A, G, S, and C) at Tyr-93 were compromised, the Y93W mutants responded well to ACh and in most other ways were like wild-type α7, with the ACh co-application being required for PNU-120596 activation and ACh co-application increasing responses to GAT107 (data not shown). GAT107-primed potentiation was also robust with α7Y93W receptors (data not shown).

As noted above, direct activation by GAT107 was greatly increased in α7W55Y (Table 3) and was decoupled from orthosteric activation. The direct activation of W55Y mutants was so increased and protracted that any primed potentiating activity was essentially masked by the residual effects of the GAT107, whether the GAT107 was applied alone or co-applied with ACh (data not shown). Similar results were obtained when the W55Y mutation was combined with the Y93W mutation.

As with the single α7Trp-55 mutants described, the α7W55Y,Y93W double mutant responded to the PAMs TQS and PNU-120596 as allosteric agonists. The PNU-120596-evoked responses of the double mutant were insensitive to 1 μM MLA (data not shown) but were reduced when PNU-120596 was co-applied with ACh (data not shown).

A graphic summary of our results with α7 wild-type and the Trp-55 and Tyr-93 mutants (summarized in Table 4) is provided in Fig. 13. Fig. 13 schematically represents a comparison of the ability of the receptors to respond to PNU-120596, TQS, or GAT107 applied alone or in combination with ACh (*shaded lower bars*). The relative size of the *ovals* in Fig. 13 indicates the magnitude of the receptor responses. In Fig. 13, the *green circles*, representing activation by ACh alone, are scaled 10-fold relative to the *red ovals* representing activation potentiated by the PAMs.

Mutations of Trp-55 were very effective at decoupling the orthosteric and allosteric activation sites, and the small residue substitutions at Tyr-93 compromised orthosteric activation, partially (Y93A) or completely (Y93C), but had relatively little effect on allosteric activation. However, it should be noted that the direct activation of α7Y93C by GAT107 was fundamentally different from direct activation of wild-type α7, because it was not sensitive to MLA co-application.

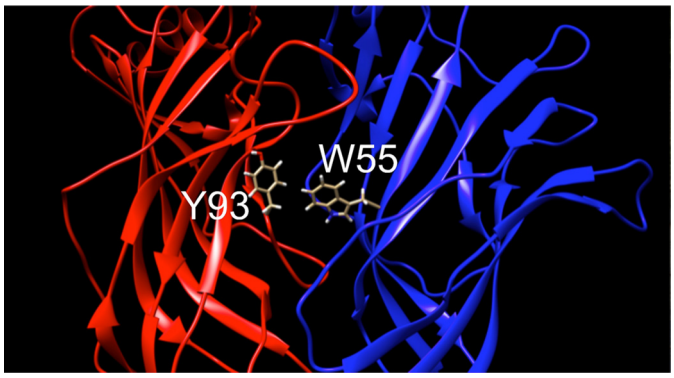

FIGURE 10. **Image showing the proximity of Tyr-93 on the primary face of the α7 agonist-binding site to Trp-55 on the complementary side.**

DISCUSSION

GAT107 has three modes of activity on wild-type α7 nAChR, two of which, primed and direct potentiation, are similar to what have been reported for other type II PAMs, except that the priming of receptors by GAT107 appears more stable than what has previously been described for other PAMs. The potentiating activity of GAT107, like that of PNU-120596, involves two modes, one of which relies on the rapid perturbation of the population of recep-

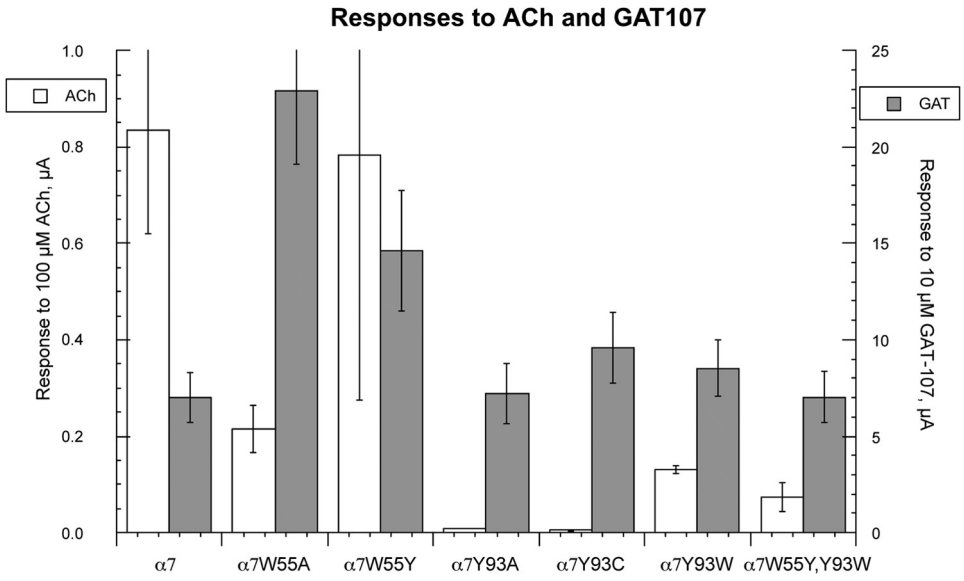

FIGURE 11. **Evaluation of functional expression of wild-type and mutant α7 nAChR based on their responses to 100 μM ACh or 10 μM GAT107 3 days after injection.** All data were obtained on the same day from the cells acquired from the same frog. Peak current data are expressed in μA, with ACh responses on the *left-hand scale* and GAT107 responses on the *right-hand scale*. Each *bar* is the average (±S.E.) of at least four oocytes. Note that the EC_{50} of α7Y93A for ACh is over 300 μM, and so the low ACh responses represent, in part, the relatively low potency of ACh for this mutant. In the case of α7Y93C, no responses to ACh at any concentration were ever above our level of detection.

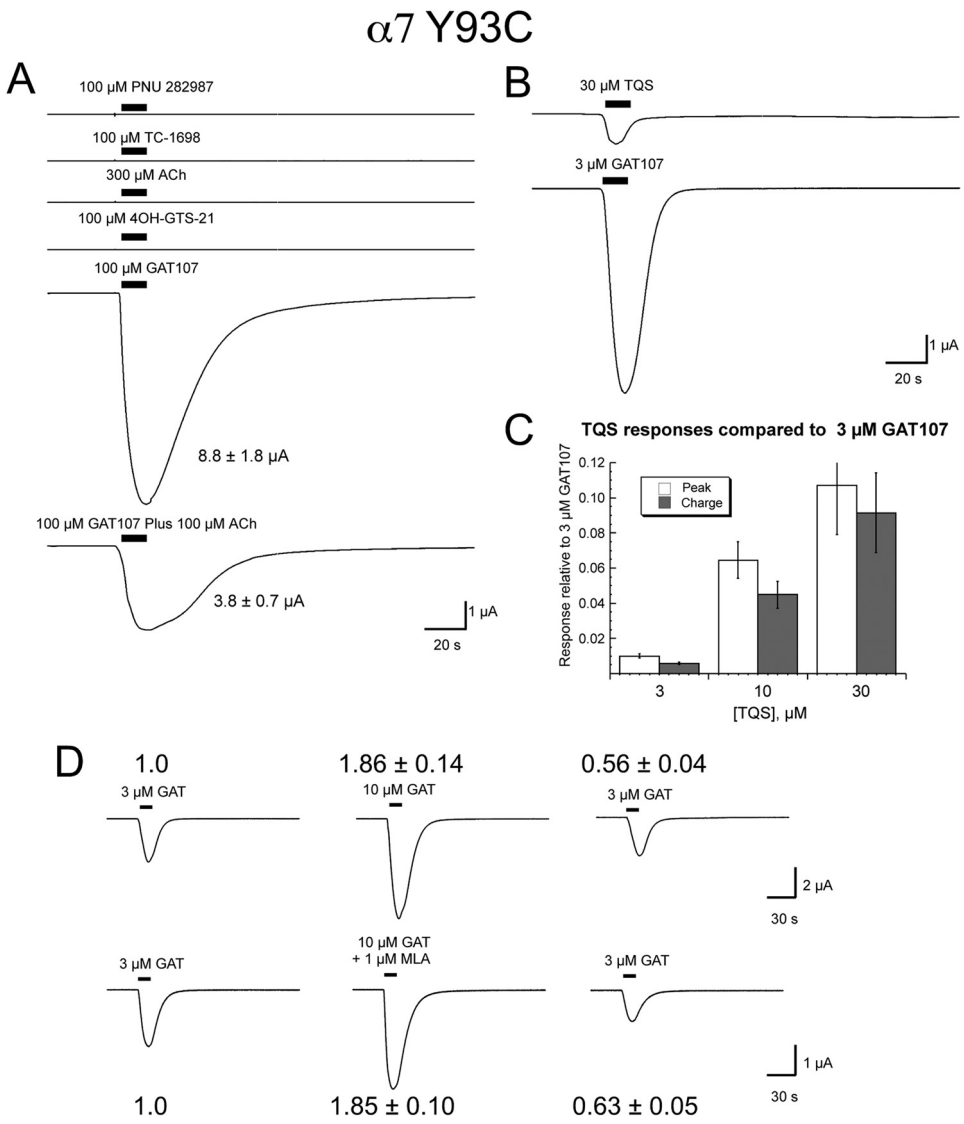

FIGURE 12. **Allosteric activation and orthosteric insensitivity of α7Y93C.** *A,* representative data from a cell expressing α7Y93C showing the failure of multiple orthosteric agonists to evoke a response, whereas GAT107 produced a large response. The response to 10 μM GAT107 was decreased when GAT107 was co-applied with 100 μM ACh. *B* and *C,* although α7Y93C receptors were not significantly activated by PNU-120596 (data not shown), they responded to relatively high concentrations of TQS, although less well than to a lower concentration of GAT107. Representative data are shown in *B*, and averaged data (± S.E.) are provided in *C*. Note, the data shown are from the Y93C mutant made in the pseudo-wild-type C116S background (see under "Materials and Methods"); Y93C mutants in the C116C wild-type background were similarly insensitive to ACh yet responded well to GAT107 (data not shown). *D,* representative traces of cells expressing α7Y93C to 10 μM GAT107 applied alone or co-applied with 1 μM MLA. Control response to 3 μM GAT107 before and after the 10 μM GAT107 applications are also shown for comparison. The values above (GAT107 applied alone) or below the traces (GAT107 co-applied with MLA) are the average peak current amplitudes of cells ($n = 7$) calculated relative to the average of two initial responses to 3 μM GAT107 alone. There were no statistically significant effects of MLA.

tors to produce synchronous transient activation, and another form that is slower to equilibrate and mostly represents the conversion of one or more desensitized states into novel conducting states (O′) that are physiologically and pharmacologically distinct from the normal conduction state (3).

The ability of GAT107 to produce direct activation of α7 nAChR distinguishes it from a prototypical PAM, inviting the designation as an ago-PAM. It was previously proposed that both the direct activation and the potentiating activity of 4BP-TQS were associated with a single binding site in the transmembrane domain. Our data suggest that this view is only partially correct and that direct activation is likely to involve either a second binding site or, less likely, a second mode of activity at a single binding site. Direct activation relies on the presence of the molecule in solution so that it can be bound in a way that involves rapid dissociation and rebinding. Direct activation is also distinct from potentiation in that it is sensitive to the co-application of MLA, whereas primed potentiation is not. Although the actual site for transducing direct activation is unknown, it is unlikely to be identical to the site for binding orthosteric agonists. The chemical nature of GAT107 bears no resemblance to the orthosteric agonist pharmacophore; it lacks the key cationic element, and the primarily noncompetitive nature of the MLA blockade is also inconsistent with activity at the orthosteric site. The data indicating rapid-on and rapid-off binding for the direct activation are suggestive of a site of action in the solvent-accessible surface of the receptor, in the extracellular domain, possibly in a position to interact with the Cys

TABLE 4
Effects of mutations at target residues

Trp-55
All mutants respond to both orthosteric agonists and GAT107
Direct activation of all Trp-55 mutants was unlike direct activation of wild type
Increased in amplitude
Increased in duration
Insensitive to co-application with MLA
Consistent with agonism based strictly on allosteric activity
Allosteric agonism is decoupled from orthosteric activation
Other PAMs (PNU-120596 and TQS) have increased activity
Can activate without co-applied orthosteric agonist
Tyr-93
Required for orthosteric activation
Y93C and Y93S are insensitive to ACh applied alone
ACh has reduced efficacy and potency on Y93A and Y93G
Not required for allosteric activation
Y93C and Y93S are sensitive to GAT107
Y93C and Y93S PAM activities increased by ACh
Allosteric activation of Y93C is MLA-insensitive
Y93W responds to orthosteric and PAMs agonists like wild type does
W55Y,Y93W
Shows additive effects of the single mutation
No compensatory effects
Orthosteric agonists decrease allosteric activation

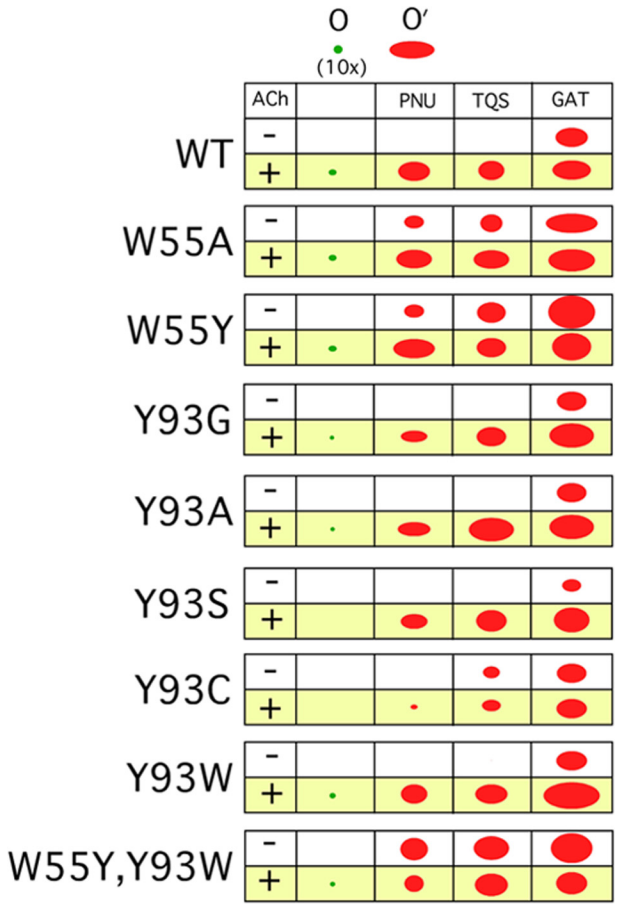

FIGURE 13. **Summary of α7 wild-type and mutant receptor sensitivity to ACh and the allosteric agents PNU-120596 (*PNU*), TQS, and GAT107 (*GAT*).** Orthosteric activation by ACh alone is represented by *small green dots*. The scale of the *green* markers is magnified ~10-fold relative to allosterically activated (in the absence of ACh) or modulated (in the presence of ACh) currents, shown in *red*. The areas of the *circles* represent the approximate relative magnitude of the net charge responses. Note that in some cases there is a negative modulation of allosteric activated currents produced by ACh, as in the case of the PNU-120596-stimulated currents of α7W55Y,Y93W nAChR (data not shown).

loop. For the reasons stated above, we propose that direct activation requires a site or mode of action distinct from the primary PAM site. Nonetheless, direct activation does rely on activity at the PAM site because interacting with the G site (Fig. 5) will necessarily permit binding to the P site as well, and the direct ion channel activation probably relies on both of these events. Because freely diffusible binding can occur on the scale of nanoseconds, binding at the G site probably happens much more rapidly than at the P site. However, the time sensitivity of our recording/detection system is on the time scale of seconds, which would be long enough for binding to occur at the P site.

The binding of PAMs, presumably at sites within the transmembrane domain, enables the receptor to manifest a very stable (O′) conducting state(s) that appears to derive from a desensitized state that is unique to α7. With ordinary PAMs the activation of these states requires coupling with the orthosteric binding site in a manner that is more stable and may be associated with higher levels of agonist occupancy than that which most effectively promotes the normal short lived O* conducting state (3). It may be the case, therefore, that PAM activity affects cooperative movements between or among the subunits.

Our data show that the coupling between the sites for receptor potentiation and orthosteric activity relies on Trp-55, such that the Trp-55 mutants do not require orthosteric ligands for full activation by GAT107 or high concentrations of the related compound TQS and have greatly reduced coupling with PNU-120596. These effects appear to decouple activity at the P site from requiring activity at either the G or the "A" sites because the allosteric agonist activity of the Trp-55 mutant is MLA-insensitive.

Our data show that the Y93C mutation also allows GAT107, and to a lesser degree TQS, to manifest allosteric agonism (activation not requiring orthosteric ligands); however, this appears to be due to a disruption of the function of the orthosteric binding site. Our data further show that, although Trp-55 and Tyr-93 may be proximal to one another across the subunit interface, coupling of orthosteric and allosteric activities is unlikely to rely on a directly reciprocal interaction between these residues, at least to the extent that reversal of the amino acids Tyr and Trp did not normalize receptor function, but rather, the double mutant showed effects that were more additive than compensatory.

The location of these key aromatic amino acids at the subunit interface proximal to the orthosteric binding site is consistent with both control (*i.e.* orthosteric) and potentiated activation requiring cooperative effects among the subunits, with allosteric agents able to convert cooperativity that is negative in regard to channel activation under control conditions (in the absence of a PAM) into cooperativity that is positive for channel activation. The question as to what degree do all of the subunits have to work in concert to achieve these effects is difficult to address because the dynamic energetic landscape of both control and potentiated receptors involves both PAM-sensitive (D_s) and PAM-insensitive (D_i) states (3). Although high levels of PAM and orthosteric agonist binding can promote large transient activation, they also promote more rapid equilibration that favors the D_i state. It would be useful to know to what

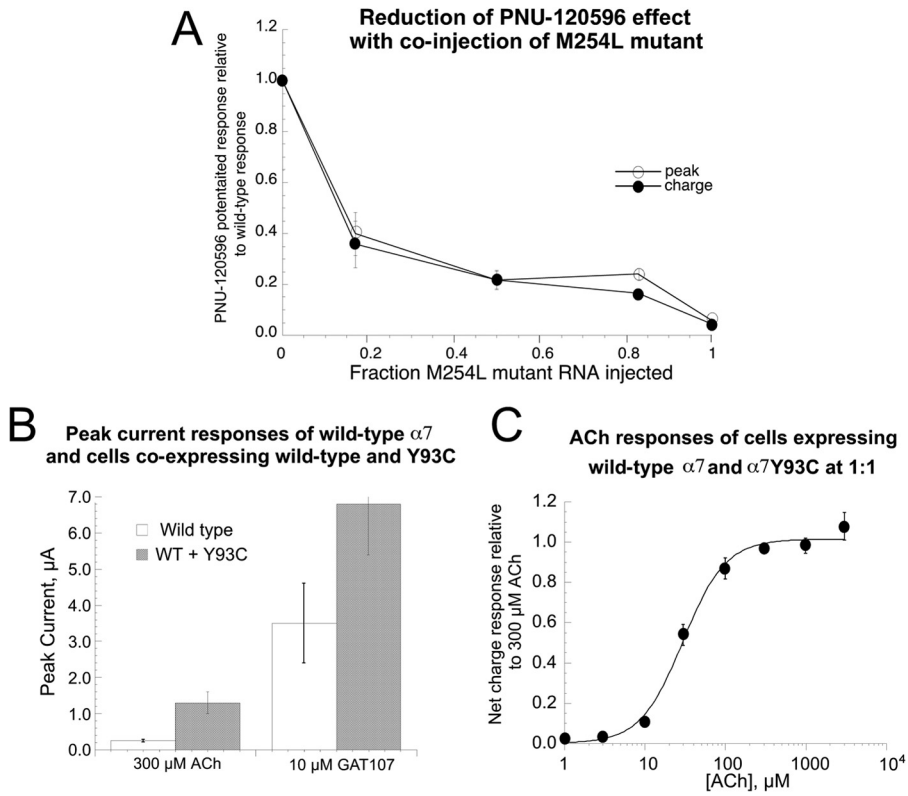

FIGURE 14. *A,* fractional expression of the PAM-insensitive M254L mutant effects on currents evoked by the co-application of 10 μM ACh and 30 μM PNU-120596 on human α7 expressed in oocytes. Note that when the mutant was co-expressed at a ratio of 1:5 (17%), there was a 60% reduction in the potentiated response. At this low ratio, the 40% residual response corresponds to the predicted fraction of receptors that would contain only wild-type subunits, consistent with the hypothesis that a single mutated subunit is sufficient to eliminate all potentiation. *B,* peak current responses of cells expressing wild-type α7 or wild-type α7 co-expressed with α7Y93C at the RNA ratio of 1:1 to 300 μM ACh or 10 μM GAT107. All cells were from the same batch of oocytes and recorded 2 days after injection. Each *bar* represents the average responses of at least six cells (± S.E.). *C,* net charge concentration-response data for cells expressing wild-type α7 co-expressed with α7Y93C at the injected RNA ratio of 1:1. The EC_{50} for ACh was 30 ± 3 μM. Each point represents the average responses of at least six cells (± S.E.).

degree the M254L mutation, which limits PAM activity, precludes PAM binding or simply the coupling of PAM binding to the triggering effects of orthosteric agonist binding. When the M254L mutant receptor is co-expressed at a very small fraction with wild-type subunits, there is a very large suppression of potentiated activity (Fig. 14*A*). It is interesting to speculate that potentiated activity requires highly cooperative interaction among all the subunits, whereas orthosteric activity may rely on independent coupling between pairs of subunits. We have previously shown that even muscle-type receptors can be fully activated with just a single binding site available for orthosteric agonists (39). Likewise, when the ACh-insensitive Y93C mutant was co-expressed 1:1 with wild-type α7, responses to ACh measured 2 days after injection were larger ($p < 0.05$) than the ACh responses of cells injected with wild-type alone (Fig. 14*B*), and the co-expressing cells responded to ACh with potency (EC_{50} = 30 ± 3 μM, Fig. 14*C*) comparable with wild-type α7 (26).

The identification of ago-PAMs has opened up an interesting new area for the evaluation of α7-targeting therapeutic agents that bring along new challenges and opportunities for understanding α7 function *in vivo*. PAMs have well established therapeutic utility that, in most cases, is hypothesized to rely on the naturally occurring agonist as a limiting factor. The reasonably good therapeutic index for benzodiazepines, which are GABA receptor PAMs, would likely be nullified in an alternative drug that was a GABA receptor ago-PAM. In this regard, part of the course for the therapeutic development of α7 ago-PAMs will be identifying the right indications for which they will be useful.

Future structure-activity studies of ago-PAMs should endeavor to segregate the pharmacophores for direct activation and primed potentiation. In this way, we may find full and partial agonist ago-PAMs with different intrinsic efficacies and various levels of priming activity as well as find concentration-dependent tuning of the balance between these effects. It may also be interesting to determine whether specific ligands can be identified for the G-binding site that could differentially modulate PAM and ago-PAMs by increasing or antagonizing their activities, respectively.

Acknowledgments—We thank Professor Jean-Pierre Changeux and Dr. Ralph Loring for helpful discussions. OpusXpress experiments were conducted by Shehd Abdullah Abbas Al Rubaiy and Khan A. Manther.

REFERENCES

1. Le Novère, N., Corringer, P. J., and Changeux, J. P. (2002) The diversity of subunit composition in nAChRs: evolutionary origins, physiologic and pharmacologic consequences. *J. Neurobiol.* **53,** 447–456
2. Papke, R. L., Bencherif, M., and Lippiello, P. (1996) An evaluation of neuronal nicotinic acetylcholine receptor activation by quaternary nitrogen compounds indicates that choline is selective for the α7 subtype. *Neurosci. Lett.* **213,** 201–204

3. Williams, D. K., Wang, J., and Papke, R. L. (2011) Investigation of the molecular mechanism of the α7 nAChR positive allosteric modulator PNU-120596 provides evidence for two distinct desensitized states. *Mol. Pharmacol.* **80,** 1013–1032
4. Wang, H., Yu, M., Ochani, M., Amella, C. A., Tanovic, M., Susarla, S., Li, J. H., Wang, H., Yang, H., Ulloa, L., Al-Abed, Y., Czura, C. J., and Tracey, K. J. (2003) Nicotinic acetylcholine receptor α7 subunit is an essential regulator of inflammation. *Nature* **421,** 384–388
5. de Jonge, W. J., and Ulloa, L. (2007) The α7 nicotinic acetylcholine receptor as a pharmacological target for inflammation. *Br. J. Pharmacol.* **151,** 915–929
6. Thomsen, M. S., and Mikkelsen, J. D. (2012) The α7 nicotinic acetylcholine receptor ligands methyllycaconitine, NS6740 and GTS-21 reduce lipopolysaccharide-induced TNF-α release from microglia. *J. Neuroimmunol.* **251,** 65–72
7. Briggs, C. A., Grønlien, J. H., Curzon, P., Timmermann, D. B., Ween, H., Thorin-Hagene, K., Kerr, P., Anderson, D. J., Malysz, J., Dyhring, T., Olsen, G. M., Peters, D., Bunnelle, W. H., and Gopalakrishnan, M. (2009) Role of channel activation in cognitive enhancement mediated by α7 nicotinic acetylcholine receptors. *Br. J. Pharmacol.* **158,** 1486–1494
8. Taly, A., Corringer, P. J., Guedin, D., Lestage, P., and Changeux, J. P. (2009) Nicotinic receptors: allosteric transitions and therapeutic targets in the nervous system. *Nat. Rev. Drug Discov.* **8,** 733–750
9. Bencherif, M., Lippiello, P. M., Lucas, R., and Marrero, M. B. (2011) α7 nicotinic receptors as novel therapeutic targets for inflammation-based diseases. *Cell. Mol. Life Sci.* **68,** 931–949
10. Hajós, M., and Rogers, B. N. (2010) Targeting α7 nicotinic acetylcholine receptors in the treatment of schizophrenia. *Curr. Pharm. Des.* **16,** 538–554
11. Leiser, S. C., Bowlby, M. R., Comery, T. A., and Dunlop, J. (2009) A cog in cognition: how the α7 nicotinic acetylcholine receptor is geared towards improving cognitive deficits. *Pharmacol. Ther.* **122,** 302–311
12. Williams, D. K., Wang, J., and Papke, R. L. (2011) Positive allosteric modulators as an approach to nicotinic acetylcholine receptor-targeted therapeutics: Advantages and limitations. *Biochem. Pharmacol.* **82,** 915–930
13. Young, G. T., Zwart, R., Walker, A. S., Sher, E., and Millar, N. S. (2008) Potentiation of α7 nicotinic acetylcholine receptors via an allosteric transmembrane site. *Proc. Natl. Acad. Sci. U.S.A.* **105,** 14686–14691
14. Kalappa, B. I., Sun, F., Johnson, S. R., Jin, K., and Uteshev, V. V. (2013) A positive allosteric modulator of α7 nAChRs augments neuroprotective effects of endogenous nicotinic agonists in cerebral ischaemia. *Br. J. Pharmacol.* **169,** 1862–1878
15. Freitas, K., Carroll, F. I., and Damaj, M. I. (2013) The antinociceptive effects of nicotinic receptors α7-positive allosteric modulators in murine acute and tonic pain models. *J. Pharmacol. Exp. Ther.* **344,** 264–275
16. Callahan, P. M., Hutchings, E. J., Kille, N. J., Chapman, J. M., and Terry, A. V., Jr. (2013) Positive allosteric modulator of α7 nicotinic-acetylcholine receptors, PNU-120596 augments the effects of donepezil on learning and memory in aged rodents and non-human primates. *Neuropharmacology* **67,** 201–212
17. Munro, G., Hansen, R., Erichsen, H., Timmermann, D., Christensen, J., and Hansen, H. (2012) The α7 nicotinic ACh receptor agonist compound B and positive allosteric modulator PNU-120596 both alleviate inflammatory hyperalgesia and cytokine release in the rat. *Br. J. Pharmacol.* **167,** 421–435
18. Thomsen MS, El-Sayed M, and Mikkelsen JD. (2011) Differential immediate and sustained memory enhancing effects of α7 nicotinic receptor agonists and allosteric modulators in rats. *PLoS One* **6,** e27014
19. Grønlien, J. H., Håkerud, M., Ween, H., Thorin-Hagene, K., Briggs, C. A., Gopalakrishnan, M., and Malysz, J. (2007) Distinct profiles of {α} nAChR positive allosteric modulation revealed by structurally diverse chemotypes. *Mol. Pharmacol.* **72,** 715–724
20. Gill, J. K., Savolainen, M., Young, G. T., Zwart, R., Sher, E., and Millar, N. S. (2011) Agonist activation of {α}7 nicotinic acetylcholine receptors via an allosteric transmembrane site. *Proc. Natl. Acad. Sci. U.S.A.* **108,** 5867–5872
21. Thakur, G. A., Kulkarni, A. R., Deschamps, J. R., and Papke, R. L. (2013) Expeditious synthesis, enantiomeric resolution and enantiomer functional characterization of (4-(4-bromophenyl)-3a,4,5,9b-tetrahydro-3*H*-cyclopenta[c]quinoline-8-sulfonamide (4BP-TQS) an allosteric agonist–positive allosteric modulator of α7 nAChR. *J. Med. Chem.* **56,** 8943–8947
22. Kulkarni, A. R., and Thakur, G. A. (2013) Microwave-assisted expeditious and efficient synthesis of cyclopentene ring-fused tetrahydroquinoline derivatives using three-component povarov reaction. *Tetrahedron Lett.* **54,** 6592–6595
23. Papke, R. L., Stokes, C., Williams, D. K., Wang, J., and Horenstein, N. A. (2011) Cysteine accessibility analysis of the human α7 nicotinic acetylcholine receptor ligand-binding domain identifies L119 as a gatekeeper. *Neuropharmacology* **60,** 159–171
24. Papke, R. L., and Stokes, C. (2010) Working with OpusXpress: methods for high volume oocyte experiments. *Methods* **51,** 121–133
25. Halevi, S., Yassin, L., Eshel, M., Sala, F., Sala, S., Criado, M., and Treinin, M. (2003) Conservation within the RIC-3 gene family. Effectors of mammalian nicotinic acetylcholine receptor expression. *J. Biol. Chem.* **278,** 34411–34417
26. Papke, R. L., and Porter Papke, J. K. (2002) Comparative pharmacology of rat and human α7 nAChR conducted with net charge analysis. *Br. J. Pharmacol.* **137,** 49–61
27. Brejc, K., van Dijk, W. J., Smit, A. B., and Sixma, T. K. (2002) The 2.7 Å structure of AChBP, homologue of the ligand-binding domain of the nicotinic acetylcholine receptor. *Novartis Found. Symp.* **245,** 22–29
28. Williams, D. K., Peng, C., Kimbrell, M. R., and Papke, R. L. (2012) The intrinsically low open probability of α7 nAChR can be overcome by positive allosteric modulation and serum factors leading to the generation of excitotoxic currents at physiological temperatures. *Mol. Pharmacol.* **82,** 746–759
29. Wang, J., Horenstein, N. A., Stokes, C., and Papke, R. L. (2010) Tethered agonist analogs as site-specific probes for domains of the human α7 nicotinic acetylcholine receptor that differentially regulate activation and desensitization. *Mol. Pharmacol.* **78,** 1012–1025
30. Peng, C., Kimbrell, M. R., Tian, C., Pack, T. F., Crooks, P. A., Fifer, E. K., and Papke, R. L. (2013) Multiple modes of α7 nAChR non-competitive antagonism of control agonist-evoked and allosterically enhanced currents. *Mol. Pharmacol.* **84,** 459–475
31. Sitzia, F., Brown, J. T., Randall, A. D., and Dunlop, J. (2011) Voltage- and temperature-dependent allosteric modulation of α7 nicotinic receptors by PNU120596. *Front. Pharmacol.* **2,** 81
32. Bertrand, D., Bertrand, S., Cassar, S., Gubbins, E., Li, J., and Gopalakrishnan, M. (2008) Positive allosteric modulation of the α7 nicotinic acetylcholine receptor: ligand interactions with distinct binding sites and evidence for a prominent role of the M2-M3 segment. *Mol. Pharmacol.* **74,** 1407–1416
33. Corringer, P. J., Bertrand, S., Bohler, S., Edelstein, S. J., Changeux, J. P., and Bertrand, D. (1998) Critical elements determining diversity in agonist binding and densensitization of neuronal nicotinic acetylcholine receptors. *J. Neurosci.* **18,** 648–657
34. Horenstein, N. A., McCormack, T. J., Stokes, C., Ren, K., and Papke, R. L. (2007) Reversal of agonist selectivity by mutations of conserved amino acids in the binding site of nicotinic acetylcholine receptors. *J. Biol. Chem.* **282,** 5899–5909
35. Williams, D. K., Stokes, C., Horenstein, N. A., and Papke, R. L. (2009) Differential regulation of receptor activation and agonist selectivity by highly conserved tryptophans in the nicotinic acetylcholine receptor binding site. *J. Pharmacol. Exp. Ther.* **330,** 40–53
36. Stewart, D. S., Chiara, D. C., and Cohen, J. B. (2006) Mapping the structural requirements for nicotinic acetylcholine receptor activation by using tethered alkyltrimethylammonium agonists and antagonists. *Biochemistry* **45,** 10641–10653
37. Akk, G. (2001) Aromatics at the murine nicotinic receptor agonist binding site: mutational analysis of the αY93 and αW149 residues. *J. Physiol.* **535,** 729–740
38. Gay, E. A., Giniatullin, R., Skorinkin, A., and Yakel, J. L. (2008) Aromatic residues at position 55 of rat α7 nicotinic acetylcholine receptors are critical for maintaining rapid desensitization. *J. Physiol.* **586,** 1105–1115
39. Williams, D. K., Stokes, C., Horenstein, N. A., and Papke, R. L. (2011) The effective opening of nicotinic acetylcholine receptors with single agonist binding sites. *J. Gen. Physiol.* **137,** 369–384

The Activity of GAT107, an Allosteric Activator and Positive Modulator of α7 Nicotinic Acetylcholine Receptors (nAChR), Is Regulated by Aromatic Amino Acids That Span the Subunit Interface

Roger L. Papke, Nicole A. Horenstein, Abhijit R. Kulkarni, Clare Stokes, Lu W. Corrie, Cheol-Young Maeng and Ganesh A. Thakur

J. Biol. Chem. 2014, 289:4515-4531.
doi: 10.1074/jbc.M113.524603 originally published online December 20, 2013